



# Nondestructive Evaluation of Bituminous Compaction Uniformity Using Rolling Density

---

November 2017

Lev Khazanovich, PhD  
Kyle Hoegh, PhD  
Ryan Conway  
Shongtao Dai, PhD, PE

*University of Minnesota  
Minnesota Department of Transportation*

## Acknowledgments

This work was sponsored by the Federal Highway Administration (FHWA) in cooperation with the American Association of State Highway and Transportation Officials. The work was conducted as part of implementing the resulting solutions of the second Strategic Highway Research Program (SHRP2). The project was managed by Steve Cooper, SHRP2 Renewal Pavement Engineer Office of Technical Services, FHWA Resource Center. The research reported herein was performed by CH2M HILL, Inc. (CH2M), ARA, Inc., and the University of Minnesota. The authors would like to thank Dr. Derek Tompkins, Mr. Mugurel Turos, and graduate students at the University of Minnesota for their help in data collection and report preparation. Special thanks are extended to Mr. Robert Rea from the Nebraska Department of Transportation; Mr. Dale Peabody and Mr. Richard Bradbury from the Maine Department of Transportation for their help in organizing demonstration projects; and personnel of the Minnesota, Maine, and Nebraska Departments of Transportation assisting in the demonstration projects.

# Contents

Section	Page
<b>Definitions .....</b>	<b>v</b>
<b>1.0 Introduction .....</b>	<b>1</b>
<b>2.0 Background .....</b>	<b>3</b>
<b>3.0 Improvements of Rolling Density Meter and Survey Methodology .....</b>	<b>6</b>
3.1 Improvements of Rolling Density Meter Equipment.....	6
3.1.1 Equipment Precision and Accuracy.....	7
3.1.2 Improvements in Onboard Software .....	11
3.2 Development of Recommended Survey Protocol .....	11
3.2.1 Selection of Rolling Density Meter Sensor Spacing .....	12
3.2.2 Survey Patterns .....	12
3.2.3 Recommended Core Collection .....	13
3.2.4 Dielectric Constant Measurement at the Core Location .....	14
3.2.5 Survey and Project File Organization .....	14
3.3 Location Assurance and Position .....	14
<b>4.0 Demonstration Projects.....</b>	<b>15</b>
4.1 HWY 52 near Zumbrota, Minnesota .....	16
4.1.1 Section 1: Standard Asphalt Binder Content and Four-Roller Passes .....	16
4.1.2 Section 2: Increased Asphalt Binder Content and Four-Roller Passes .....	21
4.1.3 Section 3: Standard Asphalt Binder Content and Five-Roller Passes .....	24
4.1.4 Section 4: Increased Asphalt Binder Content and Five-Roller Passes .....	25
4.1.5 Compaction Uniformity Analysis .....	27
4.1.6 Conclusions .....	34
4.2 U.S. Route 1 Cherryfield, Maine .....	34
4.3 HWY 2 near Lincoln, Nebraska.....	39
4.4 HWY 9 near Clifton, Maine .....	42
4.5 I-95 NEAR Pittsfield, Maine.....	46
4.6 HWY 14 near Eyota, Minnesota.....	52
<b>5.0 Conclusions and Recommendations.....</b>	<b>60</b>
<b>6.0 References .....</b>	<b>62</b>

## Appendix

### A Test Protocol for the Rolling Density Meter

#### Tables

Table 1. Swerve Test Results for the First Generation RDM Sensors .....	10
Table 2. Swerve Test Results for the Second Generation RDM Sensors.....	11
Table 3. Section 1 Paving Summary .....	17
Table 4. Section 1 Cores.....	18
Table 5. Section 2 Paving Summary .....	21
Table 6. Section 2 Core Information .....	22
Table 7. Section 3 Paving Summary .....	24
Table 8. Section 3 Core Information .....	25
Table 9. Section 4 Paving Summary .....	26
Table 10. Section 4 Core Information .....	26
Table 11. Cherryfield, Maine Basic Survey Statistics .....	36
Table 12. Clifton, ME Basic Survey Statistics.....	46
Table 13. Pittsfield, Maine Basic Survey Statistics .....	51
Table 14. Total Core Summary for Eyota, Minnesota Project .....	53
Table 15. Mean and Median Dielectrics for Mid-lanes and Joints.....	57
Table 16. Mean and Median Air Void Contents for Mid-lanes and Joints.....	57

#### Figures

Figure 1. Rolling Density Meter .....	2
Figure 2. Three-sensor Rolling Density Meter Configuration via Extended Cart.....	6
Figure 3. Short-term Dielectric Stability Measurements for Rolling Density Meter Antennas .....	8
Figure 4. Mid-term Stability Measurements.....	9
Figure 5. Swerve Testing .....	10
Figure 6: Rolling Density Meter Surveying Behind Final Roller.....	17
Figure 7. Core Measured Air Void vs. Ground Penetrating Radar Dielectrics for Section 1 .....	20
Figure 8. Core Measured Air Void vs. Ground Penetrating Radar Dielectrics for Individual Lifts of Section 1 .....	20
Figure 9. Section 2 Correlation Model .....	23
Figure 10. Correlation Model for the Wear Lift of Section 2 .....	24
Figure 11. Section 3 Correlation Model .....	25
Figure 12. Section 4 Correlation Model .....	27
Figure 13. Real-time Data Visualization and Comparison with Cores .....	28
Figure 14. Frequency Distributions of Measured Dielectrics along HWY 52, Section 1 .....	29
Figure 15. Variation of Measured Dielectric along HWY 52, Section 1.....	30
Figure 16. Correlation Model for All Wear Lifts.....	31
Figure 17. Frequency Distributions of Measured Air Void Content along HWY 52, Section 1 .....	31
Figure 18. Variation of Measured Air Void Content, Section 1.....	32
Figure 19. Dielectric, Temperature and Roller Speed [A] Rolling Density Meter Dielectrics, [B] Paver Speed, and [C] Infrared Scanner Measured Pavement Temperature .....	33
Figure 20. Cherryfield, Maine Calibration Model .....	35

Figure 21. U.S. Route 1 Air Voids Determined from Rolling Density Meter Survey .....	37
Figure 21. U.S. Route 1 Air Voids Determined from Rolling Density Meter Survey (continued).....	38
Figure 22. Lincoln, Nebraska Calibration Model .....	40
Figure 23. Air Voids Content Heat Maps and Line Plots for HWY 2, Lincoln, Nebraska .....	41
Figure 24. Heat Maps and Line Plots of Dielectric Data for HWY 9 near Clifton, Maine .....	42
Figure 24. Heat Maps and Line Plots of Dielectric Data for HWY 9 near Clifton, Maine (continued) .....	43
Figure 24. Heat Maps and Line Plots of Dielectric Data for HWY 9 near Clifton, Maine (continued) .....	44
Figure 25. Clifton, Maine Calibration Model.....	45
Figure 26. Dielectric Maps from Joint Surveys of I-95 near Pittsfield, Maine.....	47
Figure 26. Dielectric Maps from Joint Surveys of I-95 near Pittsfield, Maine (continued).....	48
Figure 27. Dielectric Maps from Joint Surveys of I-95 near Pittsfield, Maine.....	49
Figure 27. Dielectric Maps from Joint Surveys of I-95 near Pittsfield, Maine (continued).....	50
Figure 28. Pittsfield, Maine Calibration Model .....	51
Figure 29. Eyota, Minnesota Calibration Model for All Cores .....	55
Figure 30. Core Measured Air Voids vs. Ground Penetrating Radar Dielectrics for Individual Sections of HW14 .....	56
Figure 31. Frequency Distributions of the Rolling Density Meter-measured Dielectric Constants for HWY 14 Sections near Eyota, Minnesota.....	59
Figure 32. Frequency Distributions of the Rolling Density Meter -measured Air Void Contents for HWY 14 Sections near Eyota, Minnesota.....	60

## Definitions

°F	degrees Fahrenheit
AASHTO	American Association of State Highway and Transportation Officials
AC	
ASTM	American Society for Testing and Materials
CH2M	CH2M HILL, Inc.
CL	center of the lane
DOT	Department of Transportation
EB	eastbound
FHWA	Federal Highway Administration
ft	feet/foot
ft/min	feet per minute
GHz	gigahertz
GPR	ground penetrating radar
GPS	global positioning system
GSSI	Geophysical Survey Systems, Inc.
HMA	hot mix asphalt
HWY	Highway
I	Inner (lane)
I-95	Interstate 95
IC	Intelligent Compaction
IR	infrared
mm	millimeter
MnDOT	Minnesota Department of Transportation
N	Non-wear (lift)
N/A	not applicable
NDT	Non-destructive testing
O	Outer (lane)
QA	quality assurance
QC	quality control

R <sup>2</sup>	coefficient of determination
RDM	rolling density meter
SHRP2	second Strategic Highway Research Program
SHRP2 R06C	SHRP2 Report S2-R06C-RR-1 (Sebesta et al., 2013)
STA	Station
W	Wear (lift)
WB	westbound

## 1.0 Introduction

Past research has shown that the performance of hot mix asphalt (HMA) concrete is highly dependent on the air void content of the compacted HMA pavement layer. The air void content has been shown to correlate with key HMA characteristics, such as stiffness (Bonnaure, et al., 1977), strength (Pellinen et al., 2004), and dynamic modulus (Witczak and Fonseca, 1996). Kassem, et al. (2012) found that increased air void content correlated with the increased occurrence of various pavement distresses including excessive aging and moisture damage that negatively impacted long-term performance. The impacts on long-term performance were quantified in a study performed by Linden et al. (1989), that estimated that each 1 percent increase in air voids over 7 percent lead to an approximately 10 percent reduction in pavement life.

Typically, HMA compaction is assessed using coring, which is destructive, expensive, time consuming, and limited in coverage. While these measurements are useful for post-construction analysis and are often used as primary components of quality assurance (QA) measurements, they cannot provide real-time feedback during the paving operation. The issues associated with traditional compaction measurements create a need for non-destructive methods that can collect data continuously, cheaply, and quickly.

Ground penetrating radar (GPR) provides a nondestructive testing alternative that allows for walk-behind or vehicle-mounted measurements (Evans et al., 2008; Lai et al., 2014). While these studies show the potential of new technology for improved QA in selected locations, the focus of the present study is on how a stable compaction assessment can be achieved in full-scale implementation.

The GPR equipment used in this study, the rolling density meter (RDM), is based on a system that evolved from recent research conducted under the National Academies of Science sponsored second Strategic Highway Research Program (SHRP2) (Sebesta et al., 2013). The RDM system uses specially-designed GPR sensors to determine the dielectric constant of HMA. GPR data is collected by the sensors and processed using a concentrator box. The RDM onboard computer reports the dielectric constant values of the HMA surface in real time. The dielectric values can be correlated with the percent air voids and density in new pavement.



**Figure 1. Rolling Density Meter**

The SHRP2 Report S2-R06C-RR-1 (SHRP2 R06C) (Sebesta et al., 2013) demonstrated the potential of GPR for real-time feedback on the compaction of HMA. Several RDM demonstration projects were conducted as a part of the SHRP2 R06C study (Sebesta et al., 2013). The results of these demonstrations were positive and showed that GPR is a promising tool in providing real-time feedback after final mat compaction. However, the project also demonstrated the need for additional improvement of the technology to streamline data collection, processing, and evaluation.

The SHRP2 R06C study (Sebesta et al., 2013) was conducted with a single GPR antenna collecting data along a line. To perform measurements at various transverse locations within a lane, multiple passes are required which increases the survey time and, in the case of moving a lane closer, severely limits the coverage area. To address this limitation, a three-sensor version of RDM was developed by Geophysical Survey Systems, Inc. (GSSI). The GPR sensors can be spaced between 1 and 2.5 feet (ft), to cover various areas of interest, such as joints and wheel paths, in a single survey pass. This significantly increases the productivity of testing.

To take full advantage of these GPR developments, additional efforts were required to independently evaluate and facilitate implementation of this technology at the state level. This report documents the activities that build on the SHRP2 R06C research study. The primary focus of this project was to independently evaluate the RDM technology, conduct additional field trials, and develop recommendations for the surveying methodology.

## 2.0 Background

GPR uses electromagnetic waves to explore the subsurface. In the transportation infrastructure survey, GPR has been commonly used to detect free water (Al-Qadi et al., 1991), to estimate the dielectric property of pavement materials (Al-Qadi et al., 2001), to determine the layer thicknesses (Al-Qadi and Lahouar, 2005), and evaluate HMA concrete layer density (Leng, 2011; Leng et al., 2011; Shanguan and Al-Qadi, 2014 and 2015). The American Society for Testing and Materials (ASTM) standard D6432-11 provides a procedure for applying GPR for subsurface investigation.

One of the possible applications of GPR is evaluation of variability in HMA density (Scullion and Chen, 1999), through measuring of variability in the dielectric properties of the HMA layer. The dielectric response quantifies the degree to which a material stores and transmits electromagnetic energy and is related to the tendency of a material to become polarized in the presence of electromagnetic energy. The bulk dielectric response of an HMA mixture, referred to as the effective dielectric constant, is a function of the dielectric response of the individual mixture components that depends on the dielectric constant of its constituents and their volume fractions (Al-Qadi et al., 2010).

The four primary components of an HMA mixture are: filler, aggregate, binder, and air voids. At frequencies below 7 gigahertz (GHz), the average dielectric constant values of the mineral filler, aggregate, and binder range from approximately 3 to 6, while air has a dielectric constant of approximately 1 (Shang et al., 1999; Al-Qadi et al., 2010). Although aggregate type and volumetric proportion have the biggest impact on the bulk dielectric properties of the HMA mix, if the aggregate type and volumetric proportion are uniform, the primary variation in dielectric constant comes from variations in the volume of air. This makes the GPR an attractive tool for evaluating the uniformity of compaction.

Determination of dielectric properties of the HMA layer with GPR has been traditionally done through the measurement of either round-trip travel time to reflection at the depth of the HMA layer or surface reflection. The travel time approach covers a greater depth, but relies on a known thickness. However, the HMA thickness is often unknown or spatially variable. If the HMA layer is placed in several lifts or as an overlay over an existing HMA pavement, it may be difficult to separate the travel time in the individual lifts from the overall travel time of the electromagnetic signal in the HMA layer.

To determine the bulk dielectric constant of the HMA,  $\epsilon_r$ , the AC surface reflection method uses the ratio of the amplitude of the GPR signal reflection from air to the HMA surface,  $A_0$ , to the incident amplitude (represented by the reflection from the metal plate),  $A_i$ . The dielectric

constant of the surface is determined, according to Saarenketo and Scullion (2000), using the Equation 1:

$$e_r = \left( \frac{1 + \left(\frac{A_0}{A_i}\right)}{1 - \left(\frac{A_0}{A_i}\right)} \right)^2 \quad (1)$$

The advantage of this approach is that if the upper lift is sufficiently thick (thicker than 30 millimeters [mm]), then the measured AC surface reflection depends only on the properties of the upper layer.

For newly-placed HMA lift, the dielectric constant values determined from Equation 1 can be empirically related to the relative ratio of pore volume to the total volume of each specific HMA mix, because air has a lower dielectric constant than the surrounding HMA components, and the aggregate type and volumetric proportion are typically uniform (Sebesta et al., 2013; Leng and Al-Qadi 2014). Since the dielectric properties of the HMA mix depend on the dielectric properties of the mix components that vary from project to project, cores need to be taken for each new mix at locations with measured dielectric constant. The correlation between the air voids and dielectric constants plays a key role in the accuracy of the air voids predictions made using the model.

Various impulse radar versions of ground penetrating radar have shown that the dielectric properties determined from the HMA surface reflection amplitude correspond with core measured air void content (Saarenketo and Roimela, 1998; Maser and Carmichael, 2015; Al-Qadi et al., 2010). Additionally, a step frequency array-based method improves the coverage and productivity of the measurements, making it an attractive alternative to current state-of-the-practice procedures (Hoegh et al., 2015). While these studies showed the potential of new technology for improved QA in selected locations, the focus of this study is on how a stable compaction assessment can be achieved in full-scale implementation. In the case of the step-frequency array system (Scott et al., 2006), these technologies can require intensive data processing from the frequency domain or can be cost-prohibitive, while the single impulse array systems do not provide necessary coverage for widespread implementation.

There have been several field implementations of GPR for non-destructive testing (NDT) determination of air voids. The first large-scale implementation was performed in Finland from 1996 to 1997 (Saarenketo and Roimela, 1998). Recently, several state Department of Transportations (DOTs) in the United States have held trial implementations of the technology (Popik et al., 2010; Wilson and Sebesta, 2015; Hoegh et al., 2015; Maser and Carmichael, 2015).

The most notable recent evaluation of non-destructive technologies for HMA compaction assessment was conducted by Sebesta et al. (2013), as part of the SHRP2 R06C activities. Under this project, four field demonstrations of an infrared (IR) sensor bar system from MOBA Corporation and the Texas A&M Transportation Institute's 1-gGHz radar system for the

thermal and radar surveys were conducted. On three of these projects, a 2.2-GHz air-coupled GPR system from GSSI also provided radar survey data. The study showed that the computed surface dielectric values from GPR correlated well with the air voids measured on cores taken from the pavement. Therefore, GPR measurements can be converted into surface layer air voids map. The 2.2-GHz antenna was identified as the most feasible alternative compliant with the Federal Communications Commission regulations. The study also identified the need for further improvement of the GPR technology, including developing a complete package including the software needed to convert the GPR data into HMA air void data.

The correlation between the air voids and dielectric constants plays a key role in the accuracy of the air voids predictions made using the model. The correlation achieved between measured dielectric constants and air voids has been a key measure of the success of field implementations of GPR estimation of air voids. The review of past studies identified the following common practices that resulted in successful correlations between air voids and dielectric constants (Saarenketo and Roimela, 1998; Popik et al., 2010; Sebesta et al., 2013; Wilson and Sebesta, 2015; Hoegh et al., 2015):

- Survey is completed immediately after final paving.
- The thickness of the HMA lift is 1.5 inches or less.
- GPR surveys are taken directly over cores.
- Cores collected represent a full range of the surveyed dielectric constant values.
- Temperature at the time of survey is greater than 1 degree Celsius.
- Time between core GPR survey and core extraction is minimized.

The methodologies used in surveys that resulted in poor correlations between air voids and dielectric constant were also reviewed and possible causes for the poor correlations were explored. Sebesta et al. (2013) reported a poor correlation between the RDM-measured dielectric constants and air void contents for the implementation project near Woodville, Texas. However, heavy rains occurred at the mix plant and use of an experimental fiber-containing mix may have also contributed to the poor correlation. Additionally, infrared and nuclear density NDT tests performed at the project also showed no correlation with density, suggesting that the NDT versus density error is not exclusive to the GPR methods.

Maser and Carmichael (2015) reported a poor correlation between measured dielectric values and core-measured air void contents for SR 539 in Lynden, Washington. In that study, the air void content was measured from cores varied in thickness from 3 to 4.6 inches. The authors concluded that the lack of correlation between the core-measured air voids and GPR-dielectric constants was because of a combination of thicker pavement and apparent density gradients.

Despite these limitations, it can be concluded that GPR is a promising technology for HMA compaction uniformity assessment. Improvements of equipment and the test protocol, as well as additional field validations are necessary. The efforts to address these issues are presented herein.

### 3.0 Improvements of Rolling Density Meter and Survey Methodology

Based on the feedback obtained from the SHRP2 R06C study (Sebesta et al., 2013), GSSI developed an RDM. The RDM is a dielectric profiling system that uses a cart-mounted GPR technology to continuously measure HMA compaction quality. An RDM is a light cart system that can be easily propelled by a single operator (see Figure 2). Data collected at a walking speed by 2.7-GHz antennas are processed using a concentrator box. The RDM on-board computer reports the dielectric constant values of the HMA surface in real time. The dielectric values can be correlated with the percent air voids and density in the new pavement. The RDM addresses all major issues identified by the SHRP2 R06C study. However, further improvement and verification of the GPR-based tools was required. In addition, recommendations for GPR and core data collections had to be developed. The results of these efforts are summarized herein.



**Figure 2. Three-sensor Rolling Density Meter Configuration via Extended Cart**

#### 3.1 Improvements of Rolling Density Meter Equipment

During this study, continuous feedback was provided to the RDM manufacturer and numerous improvements aimed to increase the accuracy of the device, its productivity, and user friendliness

were recommended. The most important improvements of the RDM implemented by GSSI are the following:

- Improvement of precision and accuracy of measurements.
- Improvements in the onboard software.

### 3.1.1 Equipment Precision and Accuracy

Evaluation of the air void content requires more precise GPR antennas than would be acceptable for other applications. The importance of strict performance requirements was emphasized in the SHRP2 R06C report (Sebesta et al., 2013). The SHRP2 R06C study recommended adaption of Texas DOT specifications for GPR hardware used for the HMA compaction uniformity evaluation. These specifications are based largely on the GPR reflection from a large metal plate and limit such parameters as noise-to-signal ratio, and short-term and long-term variability in the measured signal amplitude. Although measuring the GPR reflection from a metal plate is an important step in determination of dielectric properties of the HMA surface (see Equation 1), it provides only an indirect assessment of a precision and bias of the GPR antenna for this type of application.

In this study, GPR antennas were evaluated based on their ability to consistently measure the dielectric properties of a block of plastic insulating material with known dielectric properties and the lack of bias in evaluation of the HMA surface dielectric properties.

The following tests were conducted:

Short-term Dielectric Testing. This test involved collection of 50 surface dielectric measurements over a plastic sheet at a rate of 15 scans per second. Figure 4 presents the results of two sets of dielectric measurement of a plastic block with dielectric constant of 2.325, using three RDM antennas. The first set of measurements was made with the first generation of RDM firmware. All three antennas measured the dielectric constant higher than the value determined using the ASTM D150-11 method. There was a significant discrepancy between the antenna measurements. These results were reported to GSSI and triggered an upgrade of the firmware. As can be observed from Figure 4, the measurements performed with the second generation of the RDM sensors resulted in a much greater precision and a lower bias in the measurements.

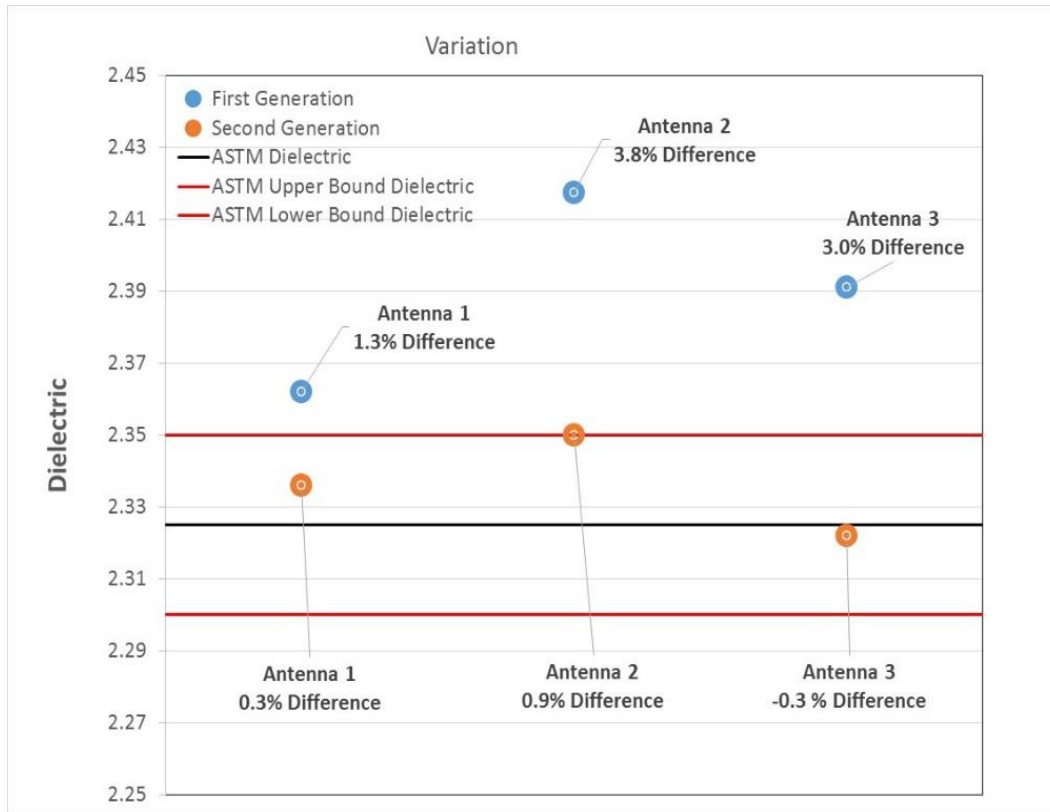


**Figure 3. Short-term Dielectric Stability Measurements for Rolling Density Meter Antennas**

Mid-term Dielectric Testing. To evaluate the stability of the measured dielectric constant over a typical data collection period, dielectric measurements were conducted over a validation block for 20 minutes continuously at a rate of 15 scans per second. Figure 5 shows the results of such measurements for one of the RDM antennas. It can be observed that the first generation of the firmware resulted in high variability of the measurements over time. While at the beginning of the testing the measured dielectric constants were about 2.3, over time some measurements resulted in dielectric constants over 2.42. The second generation of the firmware resulted in a much lower variability in the measured dielectric over time. The measured values were between 2.30 and 2.35, that is, within the range of accuracy according to ASTM D150-11 method.

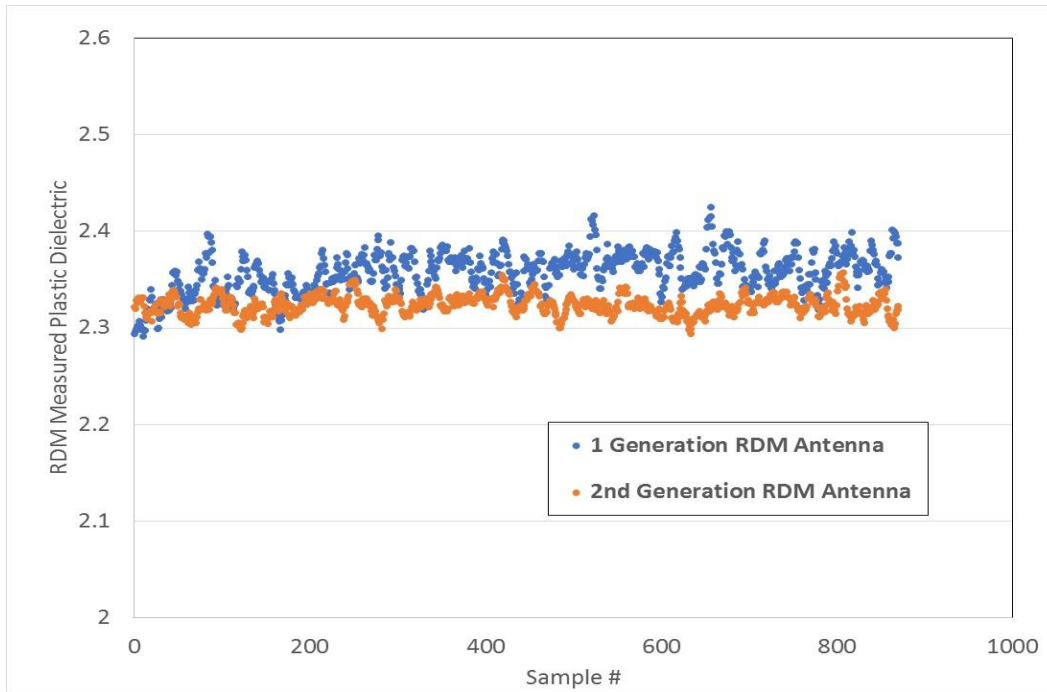


**Figure 4. Mid-term Stability Measurements**

Swerve Testing. With the three-sensor system, detection of sensor bias is important because the dielectric results should be a function of the pavement and should not be affected by which sensor was used. The GPR sensors may develop a bias for internal reasons, such as temperature gradients, or for external reasons, such as a sensor becoming unlevel or a cord interfering with the signal. To check for sensor bias, a swerve survey test was proposed. By swerving the cart along a segment of pavement (see Figure 5), the transverse discrepancies in dielectric constant values that occur because of spatial differences are “averaged out”. That is, for a survey conducted in which the cart is swerved, the averages of dielectric constants for each sensor should be approximately equal. If the sensor averages are not equal, this suggests that sensors are biased.

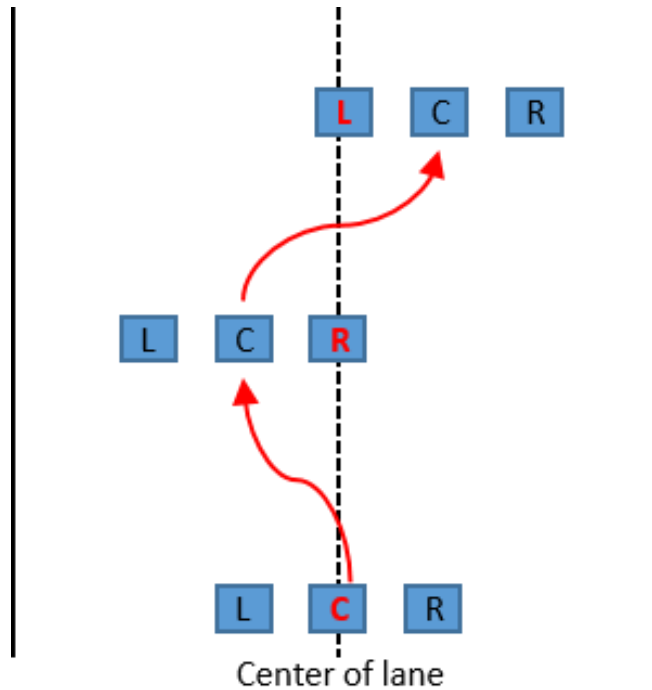


**Figure 5. Swerve Testing**

Table 1 presents an example of the results of RDM measurements collected with the first generation of RDM sensors over a 500-ft long pavement segment. A discrepancy in measured dielectrics between Sensors 2 and 3 can be observed. The mean values differ by 0.1 and the minimum and maximum values differ by 0.13 and 0.14, respectively. The differences in results between Sensors 1 and 2, as well as between Sensors 1 and 3, are much smaller.

Table 2 presents an example of the results of a swerve test for the second generation of RDM sensors. It can be observed that the discrepancy between the sensor predictions is much lower. This confirms the plastic sheet test results showing that the second generation of RDM sensors exhibit a much lower bias in the dielectric measurements.

**Table 1. Swerve Test Results for the First Generation RDM Sensors**

	Measured Dielectrics		
	RDM Sensor 1	RDM Sensor 2	RDM Sensor 3
Mean	5.52	5.57	5.47
Minimum	5.33	5.38	5.24
Maximum	5.81	5.82	5.69

**Table 2. Swerve Test Results for the Second Generation RDM Sensors**

	Measured Dielectrics		
	RDM Sensor 1	RDM Sensor 2	RDM Sensor 3
Mean	5.29	5.35	5.36
Minimum	5	5.03	5.05
Maximum	5.65	5.77	5.73

### 3.1.2 Improvements in Onboard Software

The original RDM software provided near real-time analysis of the measured dielectric values and displayed dielectric versus distance as a heat map and/or line graph making the RDM data interpretation user-friendly. However, the field trial identified the need for the onboard software improvements to simplify data organization and storage, as well as onsite data analysis. A list of recommendations was reported to GSSI and the following modifications of the onboard software have been made:

- The software provides statistical summary of the collected data (such as, frequency distribution of the computed dielectric constants, and mean and standard deviations).
- The software provides recommended core location.
- The user can organize project files by project groups.

In summary, the feedback provided to the manufacture of RDM resulted in significant improvements of the products in terms of the measurement accuracy, as well as the productivity of testing and data interpretation.

## 3.2 Development of Recommended Survey Protocol

An important part of this project was the development of a recommended test protocol including the following recommendations:

- Selection of the RDM sensor (antenna) spacing
- Survey patterns
- Selection of core locations
- Dielectric constant measurement at the core location
- Location assurance and position
- Survey and project file organization

These recommendations were developed based on the experience obtained from the field trials conducted in Minnesota, Maine, and Nebraska. The developed best-practice test protocol can be found in Appendix A. A brief summary of the developed recommendations is provided herein.

### 3.2.1 Selection of Rolling Density Meter Sensor Spacing

A 2-ft spacing between the three sensors of the RDM was implemented and is recommended for testing. The field trials and GSSI specifications suggest that the area of coverage from which the dielectric constant value is averaged is approximately a 6-inch radius circle, with locations near the center more heavily weighted. A 2-ft spacing thus leaves about 1 ft of space between the sensors that is not recorded. Surveys of transverse variation suggest that the amount variation within 1 ft is generally not significant; that is, the chances of missing a high air void region directly between the sensors are small. While a wider spacing allows greater coverage, it also increases the chance of missing a significant deviation in compaction. At full separation, the inner and outer sensors are approximately 6-ft apart and the wheel path and centerline survey can be conducted in a single pass.

### 3.2.2 Survey Patterns

An optimal survey pattern is a function of desired total survey coverage and data density. Depending on the position of the final roller in relation to the current RDM location, a survey consisting of one or three passes of RDM is recommended. If the RDM is within 1,000 ft of the final roller compactor, three RDM passes can be made for a total of nine sensor-passes. One pass should be made directly adjacent to the centerline longitudinal joint. The next pass should be conducted in the middle of the lane.

One of the field trials in Minnesota identified low joint compaction as a key issue. When there is access to a fully-formed longitudinal joint, another adjacent pass is recommended to be conducted with the closest to the joint sensor positioned 0.5 ft from the joint on its unconfined side. This positioning allows for measurement of the unconfined side of the joint after the joint is fully formed without obstructing traffic.

The total length of the survey is also an important issue. The results of this study suggest that air void content may vary greatly in the longitudinal direction; therefore, the survey should cover the full length of the paving operation. To stay near the paving operation and to limit potential data loss, surveys should be performed in segments. The experience gained from the demonstration projects in this study suggested dividing surveys into 500-ft segments. This length allows survey crew to provide more immediate feedback to the paving crew without interfering and staying within moving closure limits. Additionally, the damage done by data loss or corruption is generally limited to 500 ft. However, the optimal length may change for different locations based on the speed of the paving operation, experience of the RDM survey crew, and other factors.

### 3.2.3 Recommended Core Collection

Proper core data collection is crucial in the development of reliable air void versus dielectric constant calibration curves. The importance of collecting representative cores was discussed in the SHRP2 R06C study (Sebesta et al., 2013). In the field trials conducted under the SHRP2 R06C study, the core locations were not selected based on the measured dielectric constant value, but rather based on the thermal properties needed for IR calibration. The core data collected by this methodology were not representative of the full range of dielectric constants of the project. The protocol for outlining the collection of cores representative of the full range of survey parameters is proposed to improve the probability of producing more representative calibrations.

To ensure an even spatial distribution, the core collection spacing is specified based on the total survey length. To collect cores representative of the full range of dielectric constants encountered in the survey, maximum, minimum and intermediate values are targeted for coring. In general, high dielectric constant (high density) cores should be collected near the center of the lane, while low dielectric constant (low density) cores should be collected near the joint. For short surveys, less than 2,500 ft, collection of low, medium, and high dielectric constants is specified. For longer surveys, the project-scale variability in dielectric constant often ensures that collecting high and low dielectric value cores for each segment will result in some medium measurements in the global project, so the requirements for collecting medium dielectric constant cores is less stringent.

Efficiency is an important aspect in the selection of the core location. In the demonstration projects in Maine and Nebraska, the survey relied on post-survey analysis of dielectric constant data. The survey results were analyzed at the end of each pass, to determine the desired core locations. The survey team would then return to these locations for location marking and resurveying. While this method successfully resulted in an accurate identification of minimum and maximum dielectric constant locations, it was time consuming. The experience from the Maine project showed that it was not a practical method, unless a complete closure of traffic was available and the RDM survey crew was experienced.

A more efficient method for selecting core locations was developed and implemented during the surveys conducted in Eyota, Minnesota on Highway (HWY) 14. This method called for the marking of core locations in real time during the RDM. The basic procedure called for marking general areas of high or low compaction as they were encountered during the survey and then returning to the marked locations to record the static and dynamic core data files. Generally, the core data collection pass was substituted for the final survey pass of segment. For example, in a typical three-pass survey, potential core locations would be marked during the first two passes and then instead of the third pass, the core locations were returned to and resurveyed. This method was found to be much faster than earlier methods.

### 3.2.4 Dielectric Constant Measurement at the Core Location

The original SHRP2 methodology included resurveying of the core dielectric constant immediately before marking the core. Before the demonstration project in Zumbrota, Minnesota, it was initially hypothesized that if the core and RDM survey locations were recorded accurately enough, the dielectric constant value collected during the survey could be applied to the core measurement location without resurveying the core location. This survey method would save time during RDM surveying. However, the poor calibration results achieved for the Zumbrota, Minnesota Section 2 survey suggest that the spatial data for the cores and RDM surveys was not recorded accurately enough and that the GPR measurements must be taken directly over the core locations. This highlighted the importance of resurveying a core location before marking the core.

A protocol for resurveying the core locations was developed in this study, which takes static time-based measurements over the core location before it is marked, as well as a dynamic time-based survey around the core locations. The dynamic time-based measurement of the core dielectric constant has been found to consistently produce the best correlation between dielectric constant and air voids. This method involves conducting an approximately 6-inch survey over the core location. Both the static and dynamic surveys are conducted over 10 to 20 seconds with 10 measurements recorded per second, resulting in hundreds of dielectric constant measurements of the location and of the surrounding area. The median dielectric constant value is then calculated and used in the air voids vs dielectric constant curve.

### 3.2.5 Survey and Project File Organization

The experience gained in collecting and analyzing the data from the demonstration projects in this study showed that file organization and input standardization are crucial. Standardizing project and survey file inputs, such as the reference point used to assign transverse location and lane names, allows for consistency between projects and individual surveys even when conducted in different lanes and directions. For data analysis, files are selected based on attributes such as lift, lane, and location. By storing this crucial information in the file name, as well as within the output file itself, data can be quickly located manually or called by a program for automated data analysis.

## 3.3 Location Assurance and Position

It is very important to ensure agreement between contractor and the RDM survey measurements. Poor survey measurements result in errors in core collection and the correspondence between RDM and construction data. To ensure data agreement, a survey wheel calibration protocol was developed. This protocol checks the data agreement between the RDM survey wheel and the survey wheel used by the construction crew. The RDM survey wheel

calibration is checked on a 500-ft segment measured by the construction crew. The calibration must be within +/- 1 ft, or 99.8 percent agreement, to be accepted. Additionally, the survey crew should harmonize the RDM distance measurements with the contractor's stationing throughout the survey, to minimize error accumulation in distance measurements. Virtual reference station-corrected global positioning system (GPS) data should also be used, if possible. In addition to providing a backup for comparison with the survey wheel local positioning, the survey wheel calibration protocol was also useful in evaluating the ability of the RDM operator to stay along the specified offset from the longitudinal joint when collecting data in each 500-ft pass.

## 4.0 Demonstration Projects

This section presents the results of the RDM survey of HMA air void content conducted in this study. The primary goal of these case studies was to test the technology on real life construction projects, as well as to evaluate and improve survey methodology. The surveys were conducted in cooperation with Minnesota, Maine, and Nebraska DOTs at the following locations:

- HWY 52 near Zumbrota, Minnesota
- U.S. Route 1 near Cherryfield, Maine
- HWY 2 in Lincoln, Nebraska
- HWY 9 near Clifton, Maine
- Interstate 95 (I-95) near Pittsfield, Maine
- HWY 14 near Eyota, Minnesota

These projects represent a variety of construction techniques, HMA mix designs, and paving conditions and requirements.

The initial survey methodology was taken from the Finnish specification PANK 4122, with consideration of the recommendations from the SHRP2 R06C study (Sebesta et al., 2013). The following common steps were used in all surveys:

- At the project site, set up and initiate the RDM equipment per the manufacturer's instructions.
- Conduct airwave and metal plate calibrations. An airwave calibration involves rotating the sensors or pivoting the cart in a manner that lifts the sensors a minimum of 2 ft from the ground. A metal plate calibration involves collecting data over a metal plate.
- After placement and completion of finish rolling on the new HMA mat, collect RDM data in 500-ft long segments.
- Select core locations and collect dielectric data for these locations.

- Collect laboratory-measured air void content data and perform calibration of the air void content – dielectric constant relationship.

The survey patterns and core collection procedure varied from project to project, to accommodate specific project requirements and to account for the experience gained from the demonstration project and feedback from contractors and DOT personnel. The results of these surveys are presented in the following sections.

## **4.1 Highway 52 near Zumbrota, Minnesota**

The RDM surveys were conducted in cooperation with the Minnesota Department of Transportation (MnDOT) from May 17, 2016 to June 3, 2016. They covered approximately 5 miles of HWY 52 near Zumbrota, Minnesota. The total paving project extended from Station (STA) 896+83 to STA 1233+03 and included milling of 1.5 inches of the existing HMA surface layer and paving of two 1.5-inch-thick HMA lifts in both lanes. The project was divided by MnDOT into the following four test sections differed by the mix design and the number of roller passes:

- Section 1. A control section with a standard MnDOT HMA mix and construction practice (four roller passes).
- Section 2. An HMA mix with an increased by 0.5 percent binder content, four roller passes.
- Section 3. A standard MnDOT HMA mix, five roller passes.
- Section 4. An HMA mix with an increased by 0.5 percent binder content, five roller passes.

A description and analysis of the data collected for each section are provided herein.

### **4.1.1 Section 1: Standard Asphalt Binder Content and Four-roller Passes**

The first survey project was performed over HMA lift constructed with standard construction practices. These practices included the use of four passes of the cold roller for final compaction and an asphalt binder content of 5.2 percent. This project was conducted in eight subsections in both the inner and outer lanes and with data taken on both the wear and non-wear lift. A total of 72,968 ft of lane distance was surveyed within Section 1. A summary of all the Section 1 subsections is presented in Table 3.

**Table 3. Section 1 Paving Summary**

Date Paved	Start Stationing	End Stationing	Length (ft)	Lane	Lift
May 17, 2016	896+85	1082+21	18536	O	N
May 18, 2016	1082+21	1233+03	15082	O	N
May 20, 2016	1067+49	1180+21	11272	I	N
May 23, 2016	1180+21	1233+03	5282	I	N
May 26, 2016	896+85	973+27	7642	I	W
May 26, 2016	1048+04	1071+02	2298	I	W
June 1, 2016	1180+89	1233+03	5214	I	W
June 2, 2016	896+85	973+27	7642	O	W

Notes:

**Lane** denotes the lane (O = Outer, I = Inner).

**Lift** denotes the lift the survey was conducted on (N = Non-wear, W = Wear).

Before surveying, the RDM equipment was calibrated using the airwave and metal plate calibration procedures outlined within the GSSI user manual documentation. Surveying commenced when the paving crew had advanced approximately 1,000 ft ahead of the RDM survey crew (see Figure 7). This separation distance was chosen because it is approximately the sum of the desired section length surveyed by the RDM crew and the length of a roller pass. Maintaining this offset eliminated the interference between the RDM and paving crew. The 500-ft segment length was chosen to keep the RDM surveying practices consistent with the compaction practices. The common industry practice is to compact in approximately 500-ft segments.



**Figure 6: Rolling Density Meter Surveying Behind Final Roller**

Various survey patterns were used to explore the relationship between the data coverage and the survey time. To limit walking without data collection, only odd numbers of passes were conducted (one, three, and five). Single-pass surveys were conducted with the RDM sensor array centered in the middle of the lane, along the joint, along the shoulder, and at various points in between. Three-pass surveys included patterns that collected dense data over a particular section, such as the joint or centerline, as well as surveys that were more distributed, and collected data over the entire lane. Some of the three-pass surveys contained a swerve calibration testing, allowing for potential bias to be identified. Finally, five-pass surveys were also implemented. Like three-pass surveys, five-pass surveys provided both very dense and widely distributed data throughout the lane. Many of the five-pass surveys contained swerve calibration testing as well.

A total of 26 cores were collected for this section. Cores were collected in both the inner and outer lanes, on both lifts, and transverse offsets from 0.25 to 12 ft from the centerline. A summary of the core information is presented in Table 4. The GPR dielectric data at the core locations were correlated with the air void measurements. The results of this correlation are shown in Figure 7. Although the core data collection procedure used for Section 1 did not include resurveying of the core location, a key practice implemented in later surveys, a reasonably good fit was obtained. The coefficient of determination,  $R^2$ , of 0.6941 suggests that almost 70 percent of variation in the air void content can be explained by the model. It should be also noted that the data collected in Section 1 were taken on many different days, on different lanes, and at various weather conditions; therefore, the dielectric response may not be consistent. Figure 8 shows the calibration curves using cores collected for the non-wear and wear lifts. The fits are better for individual lifts.

**Table 4. Section 1 Cores**

Core ID	Date Paved	Core Station	Offset (ft from CL)	Lane	Lift	Air Voids
C1	May 17, 2016	1015+14	5	O	N	6.8%
C2	May 17, 2016	1015+55	1	O	N	11.3%
C3	May 17, 2016	1015+84	5	O	N	9.0%
C4	May 17, 2016	1016+79	1	O	N	9.6%
C5	May 17, 2016	1018+10	5	O	N	7.7%
C6	May 17, 2016	1018+47	1	O	N	9.8%
C7	May 17, 2016	1019+55	1	O	N	8.4%
C8	May 17, 2016	1019+75	5	O	N	8.0%
C38	May 20, 2016	1118+70	-0.25	I	N	12.1%
C39	May 20, 2016	1121+20	-0.25	I	N	12.4%
C40	May 20, 2016	1121+44	-0.25	I	N	11.5%
C41	May 20, 2016	1122+35	-0.25	I	N	12.0%

**Table 4. Section 1 Cores**

Core ID	Date Paved	Core Station	Offset (ft from CL)	Lane	Lift	Air Voids
W1	May 26, 2016	905+56	-1	I	W	4.9%
W2	May 26, 2016	905+56	-3	I	W	8.6%
W3	May 26, 2016	969+37	-5	I	W	8.7%
W5	May 26, 2016	968+95	-7	I	W	5.1%
W6	May 26, 2016	968+95	-11	I	W	10.4%
W22	June 2, 2016	907+47	0.5	O	W	8.7%
W23	June 2, 2016	907+47	4.5	O	W	5.9%
W25	June 2, 2016	913+05	4.5	O	W	7.5%
W26	June 2, 2016	911+73	-0.5	O	W	11.1%
W27	June 2, 2016	911+81	3.5	O	W	7.7%
W28	June 2, 2016	919+25	-0.5	O	W	11.5%
W29	June 2, 2016	919+25	3.5	O	W	7.4%
W30	June 2, 2016	924+02	0.5	O	W	11.2%
W31	June 2, 2016	924+02	-0.5	O	W	11.3%

Note:

CL = center of the lane

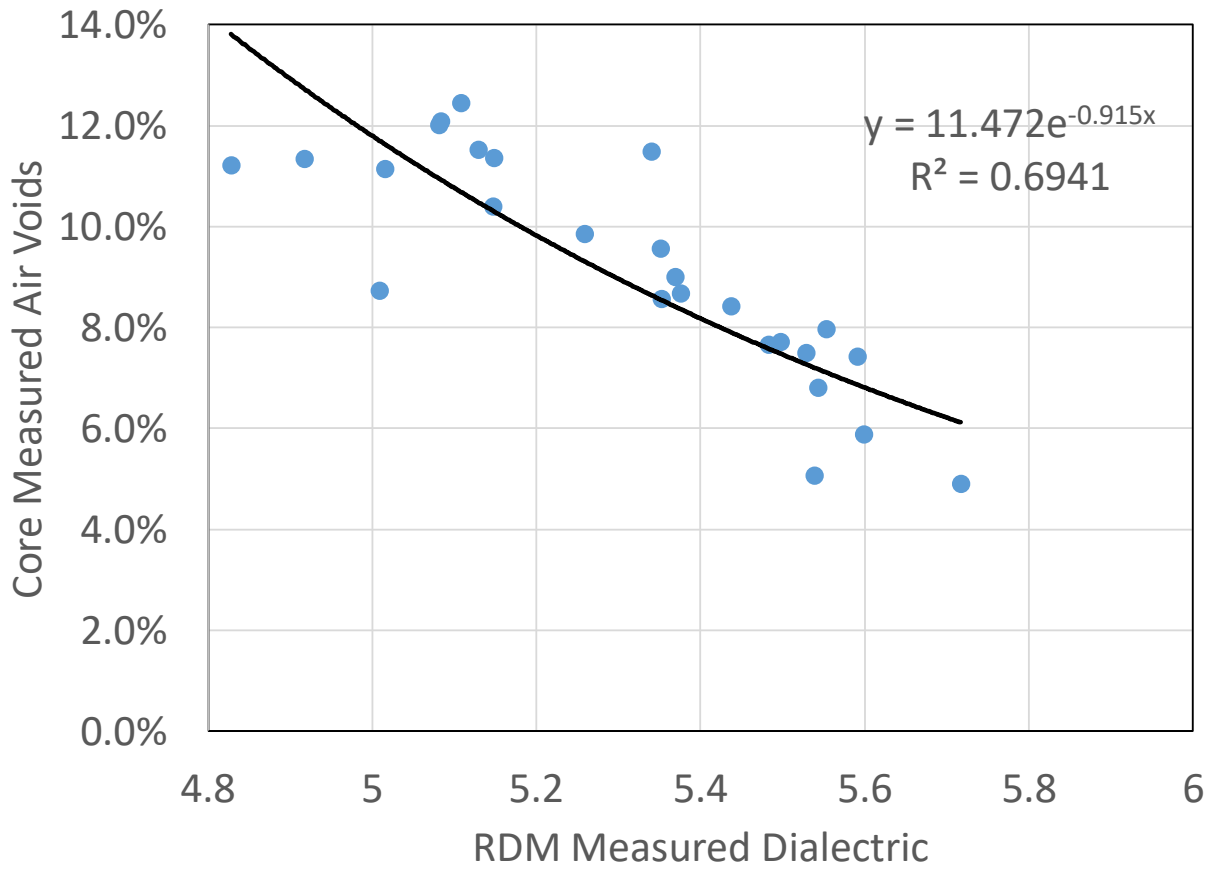


**Figure 7. Core Measured Air Void vs. Ground Penetrating Radar Dielectrics for Section 1**

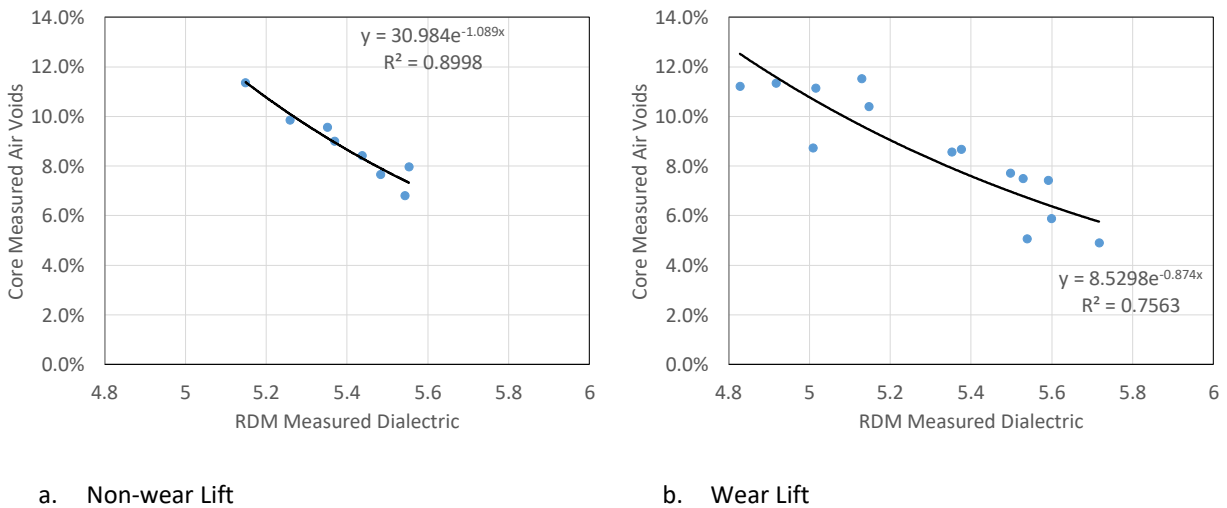


**Figure 8. Core Measured Air Void vs. Ground Penetrating Radar Dielectrics for Individual Lifts of Section 1**

#### 4.1.2 Section 2: Increased Asphalt Binder Content and Four-roller Passes

The second section was constructed with an increased asphalt binder content of 5.5 percent instead of the traditional 5.2 percent. The standard practice of four-roller passes of the cold roller was used for final compaction. This section was constructed and surveyed in four subsections: the first two were non-wearing lifts with the inner lane, the third one was the wearing lift of the inner lane, and the last subsection was the wearing lift of the outer lane. A summary of all the Section 2 subsections is presented in Table 5. A total of 27,576 ft of lane distance was surveyed within Section 2.

**Table 5. Section 2 Paving Summary**

Date Paved	Start Stationing	End Stationing	Length (ft)	Lane	Lift
May 19, 2016	897+75	1023+35	12560	I	N
May 19, 2016	1023+35	1067+49	4414	I	N
June 1, 2016	1149+64	1180+89	3125	I	W
May 26, 2016	1116+46	1233+03	7477	O	W

The GPR system, setup, and surveying procedures are the same as those used for Section 1. However, several different transverse spacings and locations were used, producing some data files that emphasized data collection at certain critical regions (such as unconfined joints), while others were more widely distributed and provided less dense information on the entire lane. The survey pattern was adjusted to match the paving speed and to collect data in areas of interest.

A total of 34 cores were collected in Section 2. They were collected in both the inner and outer lanes, on both lifts, and at transverse offsets from 0.25 to 11 ft from the centerline. While the total paved length of Section 2 is significantly shorter than Section 1, the effect of added asphalt binder was of great interest to MnDOT; therefore, cores were taken much more frequently in the non-wear lift. A summary of all the cores marked in Section 2 is presented in Table 6.

The calibration model produced for Section 2 is presented on Figure 9. As can be seen from Figure 9, the model produced a relatively poor fit. The relatively poor correlation was attributed to the lack of the RDM measurements taken directly at the core location for the majority of the cores. Figure 10 presents a calibration model produced for only the wear cores where the dielectric properties were remeasured at the core location. This subset was all paved on the same day under relatively uniform conditions and has a much better fit of the calibration model.

**Table 6. Section 2 Core Information**

Core ID	Date Paved	Core Station	Offset (ft from CL)	Lane	Lift	Air Voids
C9	May 19, 2016	905+30	1	I	N	7.3%
C10	May 19, 2016	905+30	-1	I	N	5.1%
C11	May 19, 2016	906+37	1	I	N	7.9%
C12	May 19, 2016	906+37	-1	I	N	6.0%
C13	May 19, 2016	907+97	-5	I	N	6.9%
C14	May 19, 2016	908+23	-5	I	N	5.4%
C15	May 19, 2016	908+43	-5	I	N	5.6%
C16	May 19, 2016	908+59	-5	I	N	6.8%
C17	May 19, 2016	950+78	-0.25	I	N	8.7%
C18	May 19, 2016	951+48	-0.25	I	N	6.8%
C19	May 19, 2016	952+95	-0.25	I	N	8.6%
C20	May 19, 2016	950+80	-3	I	N	6.1%
C21	May 19, 2016	954+12	-3	I	N	6.0%
C22	May 19, 2016	1008+85	-4	I	N	7.6%
C23	May 19, 2016	1010+82	-4	I	N	7.3%
C24	May 19, 2016	1011+55	-4	I	N	7.0%
C25	May 19, 2016	1012+85	-4	I	N	7.5%
C26	May 19, 2016	1012+85	-6	I	N	5.7%
C27	May 19, 2016	1013+70	-4	I	N	7.9%
C28	May 19, 2016	1013+70	-6	I	N	6.6%
C30	May 20, 2016	1050+16	-0.25	I	N	9.9%
C31	May 20, 2016	1050+19	-0.25	I	N	7.9%
C32	May 20, 2016	1050+19	-2.25	I	N	7.4%
C33	May 20, 2016	1050+34	-0.25	I	N	5.1%
C34	May 20, 2016	1053+60	-0.25	I	N	9.6%
C35	May 20, 2016	1050+34	-1	I	N	6.1%
W13	June 1, 2016	1085+66	-11	I	W	5.3%
W14	June 1, 2016	1085+33	-11	I	W	11.1%
W15	June 1, 2016	1104+30	-5	I	W	3.8%
W16	June 1, 2016	1104+04	-7	I	W	3.0%
W17	June 1, 2016	1112+63	-1	I	W	8.5%
W18	June 1, 2016	1142+63	-1	I	W	9.9%
W19	June 1, 2016	1170+41	-1	I	W	9.7%
W20	June 1, 2016	1172+72	-11	I	W	10.9%
W21	June 1, 2016	1177+60	-5	I	W	6.0%

**Table 6. Section 2 Core Information**

Core ID	Date Paved	Core Station	Offset (ft from CL)	Lane	Lift	Air Voids
W34B	June 3, 2016	1134+00	3.75	O	W	4.4%
W35	June 3, 2016	1132+01	-0.5	O	W	9.5%
W36	June 3, 2016	1137+50	1.75	O	W	4.3%
W37	June 3, 2016	1164+17	-0.5	O	W	10.1%
W38	June 3, 2016	1164+17	1.75	O	W	5.0%
W39	June 3, 2016	1162+05	-0.5	O	W	10.8%

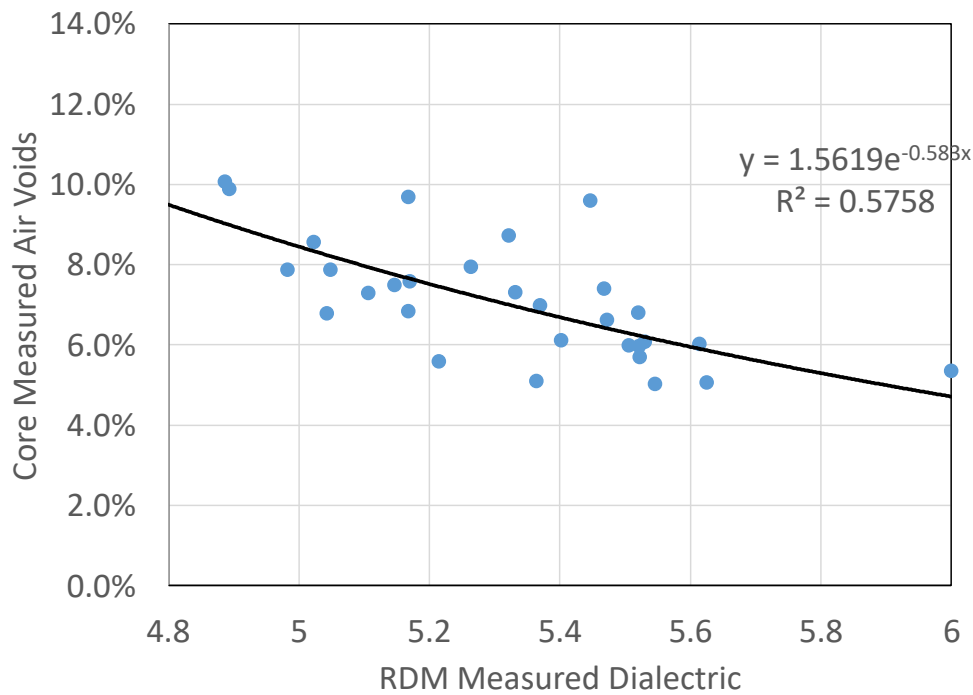


**Figure 9. Section 2 Correlation Model**

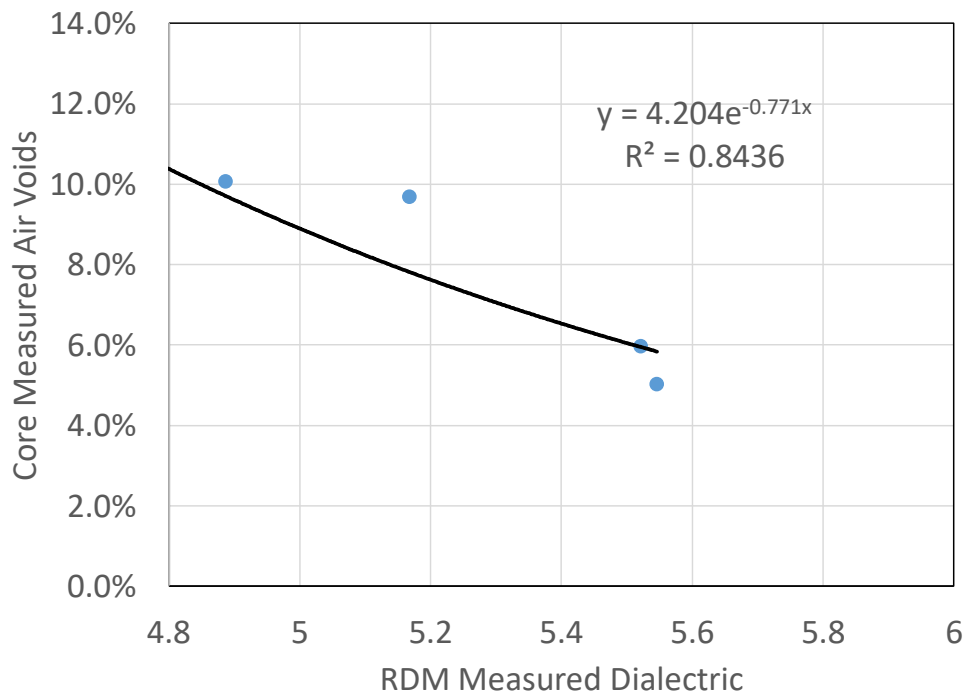


**Figure 10. Correlation Model for the Wear Lift of Section 2**

#### 4.1.3 Section 3: Standard Asphalt Binder Content and Five-roller Passes

The third survey project was performed on a section constructed with the use of five-roller passes instead of the standard four-roller passes of the cold roller used for final compaction. A standard asphalt binder content of 5.2 percent was used. The surveys were conducted on the wear lift in two subsections: one located in the inner lane and one in the outer lane as shown in Table 7. A total of 12,877 ft of lane distance was surveyed within Section 3.

**Table 7. Section 3 Paving Summary**

Date Paved	Start Stationing	End Stationing	Length (ft)	Lane	Lift
June 2, 2016	973+27	1048+04	9523	I	W
June 3, 2016	973+27	1068+50	3354	O	W

Since Section 3 was surveyed after the data collected from the surveys of Sections 1 and 2 had been analyzed, the lessons learned from the previous surveys were used to improve the core collection methodology. After the cores were marked, the dielectric properties were remeasured at the core locations. A summary of all the cores data for Section 3 is presented in Table 8.

**Table 8. Section 3 Core Information**

Core ID	Date Paved	Core Station	Offset (ft from CL)	Lane	Lift	Air Voids
W9	May 26, 2016	982+83	-1	I	W	10.3%
W10	May 26, 2016	981+87	-5	I	W	6.9%
W11	May 26, 2016	981+87	-7	I	W	4.4%
W32	June 2, 2016	981+48	4	O	W	4.8%
W33	June 2, 2016	982+45	6	O	W	4.9%

The calibration model produced for Section 3 is presented in Figure 11. As can be seen from Figure 11, the model produced a much better fit than the previous models for entire Sections 1 and 2. This improved fit was attributed to the fact that only reliable dielectric data were used in the calibration.

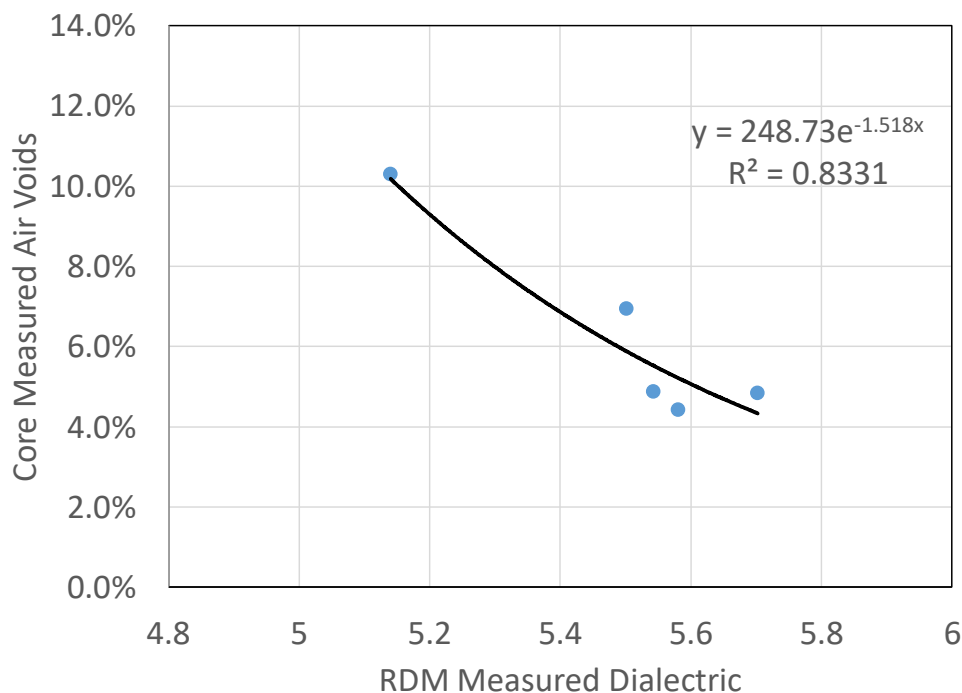


**Figure 11. Section 3 Correlation Model**

#### 4.1.4 Section 4: Increased Asphalt Binder Content and Five-roller Passes

The fourth survey project was performed over HMA layers constructed using five roller passes and an increased asphalt binder content of 5.5 percent. This section was surveyed in three subsections, as shown in Table 9, with data recorded within the inner and outer lanes on the wear lift. A total of 24,315 ft of lane distance was surveyed.

**Table 9. Section 4 Paving Summary**

Date Paved	Start Stationing	End Stationing	Length (ft)	Lane	Lift
June 1, 2016	1071+02	1149+64	7862	I	W
June 2, 2016	1068+50	1116+46	4796	O	W
June 3, 2016	1116+46	1150+00	11657	O	W

A total of nine cores were collected in Section 4. They were collected in both the inner and outer lanes at transverse offsets from 1 to 11 ft from the centerline in two of the three subsections within Section 4. An information of core locations is provided in Table 10. Like Section 3, after the cores were marked, the dielectric properties were remeasured at the core locations.

**Table 10. Section 4 Core Information**

	Core ID	Date Paved	Core Station	Offset (ft from CL)	Lane	Lift	Air Voids
1	W13	June 1, 2016	1085+66	-11	I	W	5.3%
2	W14	June 1, 2016	1085+33	-11	I	W	11.1%
3	W15	June 1, 2016	1104+30	-5	I	W	3.8%
4	W16	June 1, 2016	1104+04	-7	I	W	3.0%
5	W17	June 1, 2016	1112+63	-1	I	W	8.5%
6	W18	June 1, 2016	1142+63	-1	I	W	9.9%
7	W34B	June 3, 2016	1134+00	3.75	O	W	4.4%
8	W35	June 3, 2016	1132+01	-0.5	O	W	9.5%
9	W36	June 3, 2016	1137+50	1.75	O	W	4.3%

The calibration model produced for Section 4 is presented on Figure 12. As can be seen from Figure 12, the model produced a much better fit than the models for Sections 1 and 2. Similar to Section 3, this improved fit was because the survey crew had become more proficient at maintaining accurate location measurements when surveying and choosing cores, possibly producing a more accurate spatial association of the core and RDM locations.

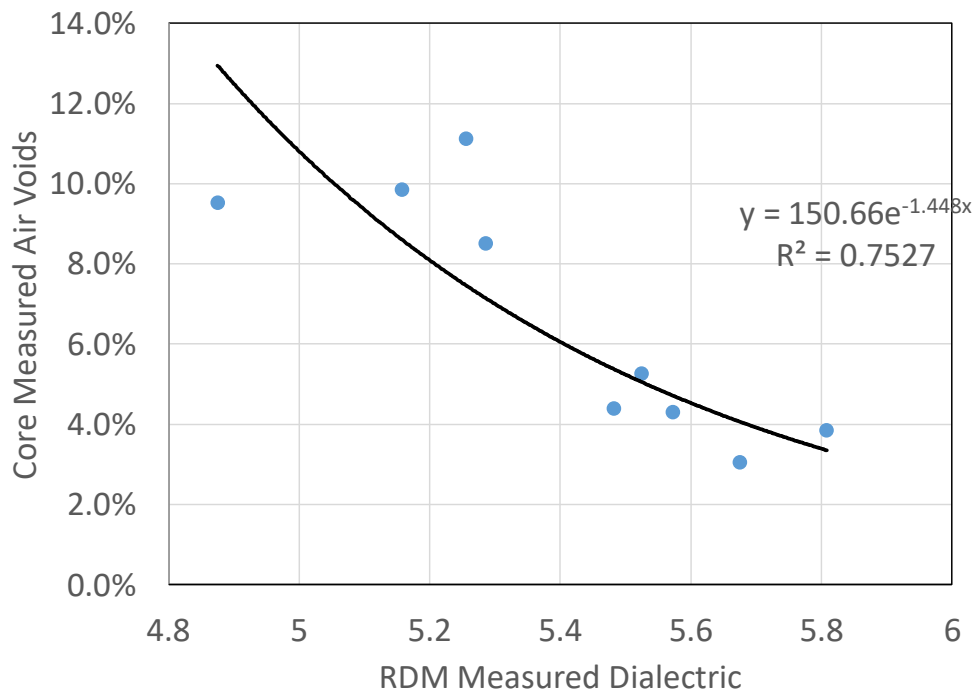
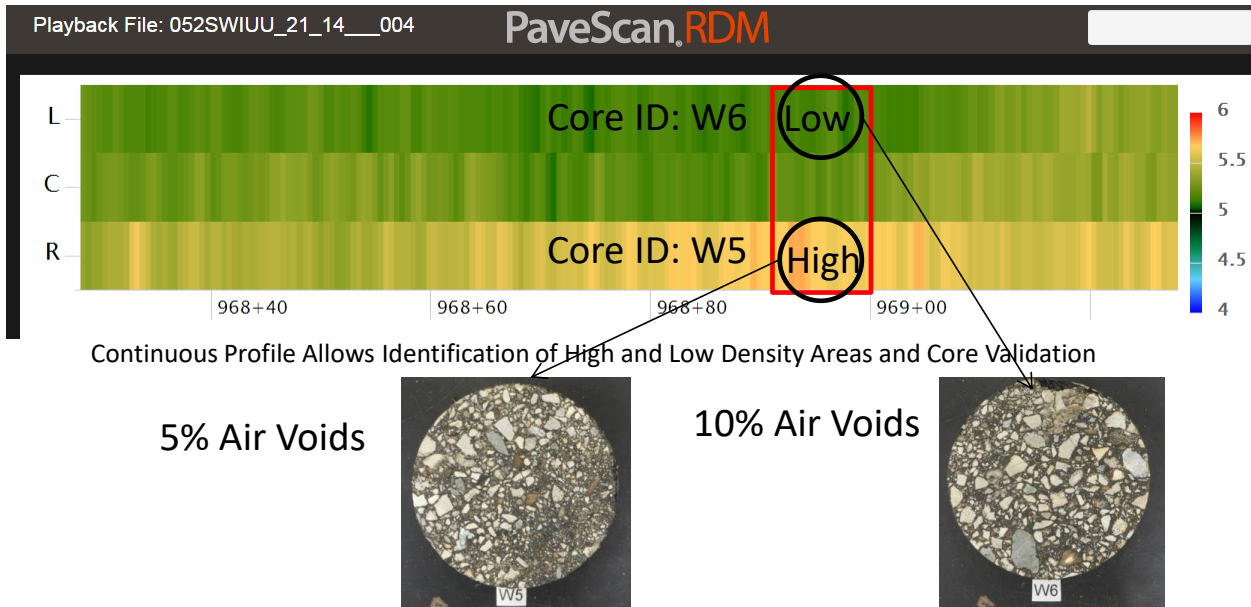


**Figure 12. Section 4 Correlation Model**

#### 4.1.5 Compaction Uniformity Analysis

One of the objectives of the Zumbrota, Minnesota demonstration project was to explore the potential of RDM use for real-time compaction uniformity evaluation. Though calibration cores must be collected to convert dielectric measurements recorded using the RDM to air void estimates, the well documented and physically-based relationship between air void content and dielectric response suggests that HMA with lower dielectric should have a higher air void content than an HMA with a higher dielectric.

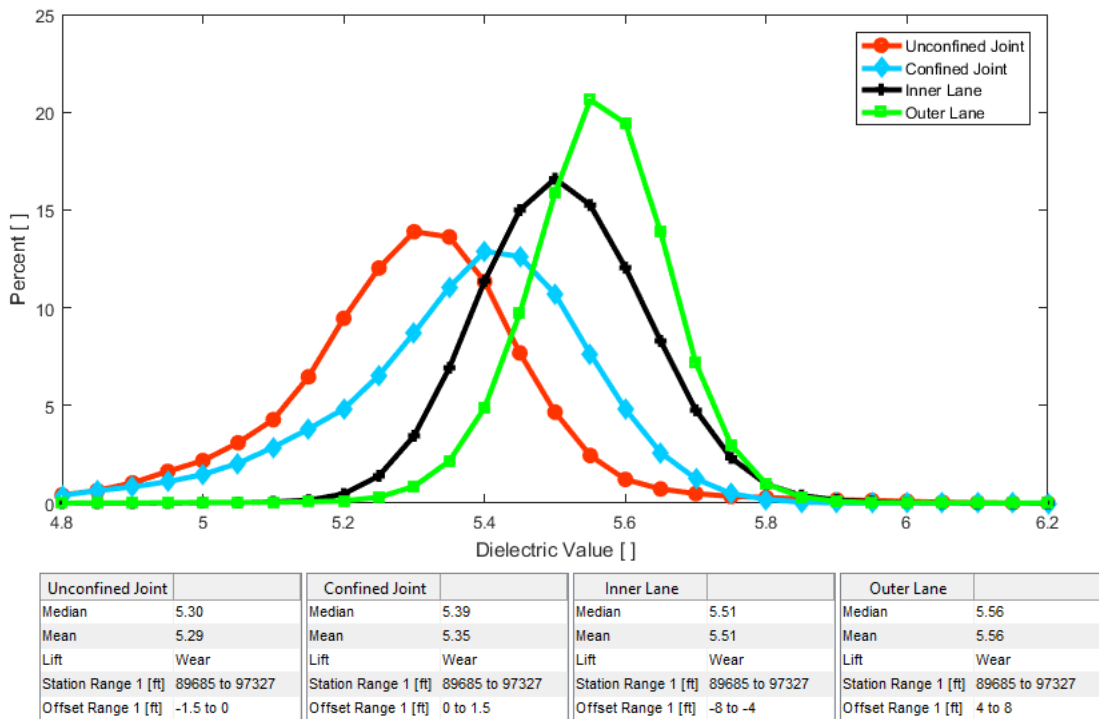
The RDM equipment displays the measured dielectric in real time during the survey. Figure 13 shows an example of a dielectric map using the software provided by the equipment manufacturer along one of the RDM passes. The areas with higher dielectric locations indicate a better compaction and the areas with lower dielectric values indicate a poorer compaction. This relative compaction map can be used to provide real-time feedback to the contractor. The laboratory air void measurements for the cores taken in these locations from the high and low compaction areas resulted in 5 percent and 10 percent, respectively, confirming the trends predicted by the RDM.



**Figure 13. Real-time Data Visualization and Comparison with Cores**

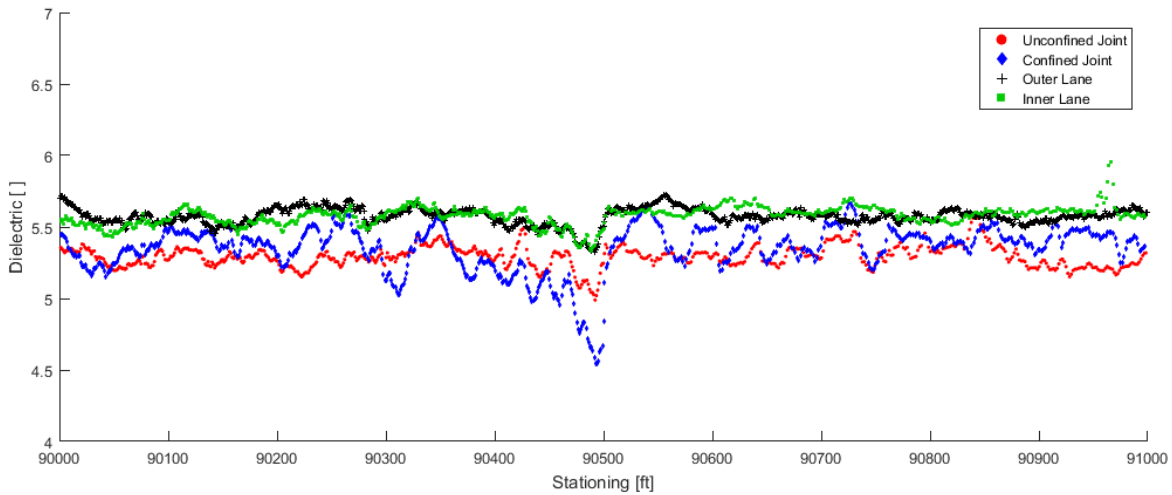
The relative achieved compaction associated with different joint confinements and lanes was investigated in this study. Figure 14 presents a frequency distribution of the measured dielectric values for wearing lift of the stretch of HWY 52 between STA 896 and STA 973. The measurements taken from 4 to 8 ft away from the longitudinal joint were considered characterizing the lane mat, while the measurements taken up to 1.5 ft away from the joint were considered characterizing joint compaction. Since the inner lane was paved before the outer lane, the outer lane side of the longitudinal joint could be compacted against the inner lane. Therefore, the outer lane side of the longitudinal joint was called confined and the inner lane side of the joint was called unconfined.

Figure 14 shows that the outer lane exhibited the highest dielectric values, closely followed by the inner lane dielectric values. The confined side of the joint has dielectric values lower than those for both lanes, but higher than the dielectrics for the unconfined side of the joint.



**Figure 14. Frequency Distributions of Measured Dielectrics along HWY 52, Section 1**

Figure 15 shows variation of the measured dielectric constants for the inner and outer lanes as well as confined and unconfined sides of the joint versus stationing for a 1,000-ft stretch of this section. As seen on Figure 15, the levels of compaction for inner and outer lanes are very similar and quite uniform. For some locations within the subsection, the confined side of the joint has higher dielectric values than the corresponding dielectric values for unconfined side of the joint and often they can be as high as the dielectrics for the inner and outer lanes. However, for other locations, the dielectric values for the confined side of the joint were significantly lower than the corresponding values for the unconfined side of the joint. This indicates that consistency of joint compaction was a problem for this stretch of the section.



	Unconfined Joint	Confined Joint	Inner Lane	Outer Lane
Median	5.31	5.41	5.58	5.59
Mean	5.29	5.34	5.57	5.57
Lift	Wear	Wear	Wear	Wear
Station Range 1 [ft]	90000 to 91000	90000 to 91000	90000 to 91000	90000 to 91000
Offset Range 1 [ft]	-1.5 to 0	0 to 1.5	-8 to -4	4 to 8

**Figure 15. Variation of Measured Dielectric along HWY 52, Section 1**

This type of analysis was used to provide real-time feedback during the Zumbrota, Minnesota project on several occasions. First, consistently low dielectric, suggesting poor compaction, was noted in locations where the roller pattern would reset. This information was passed on to the paving crew; paving was modified and the issue was resolved. On another occasion, low compaction was consistently noted in the very center of the lane. Again, the paving crew was notified and the future pavement was greatly improved.

The dielectric data were later converted to the air voids contents using a single-model calibrated with the wear lift cores from all sections shown in Figure 17 and Figure 18, which show air void content frequency distributions and variation of air voids content along the section length, respectively. As could be expected, Figure 17 shows that the outer lane has the lowest air void content and the unconfined joint has the highest percentage of area with air void content exceeding 8 percent.

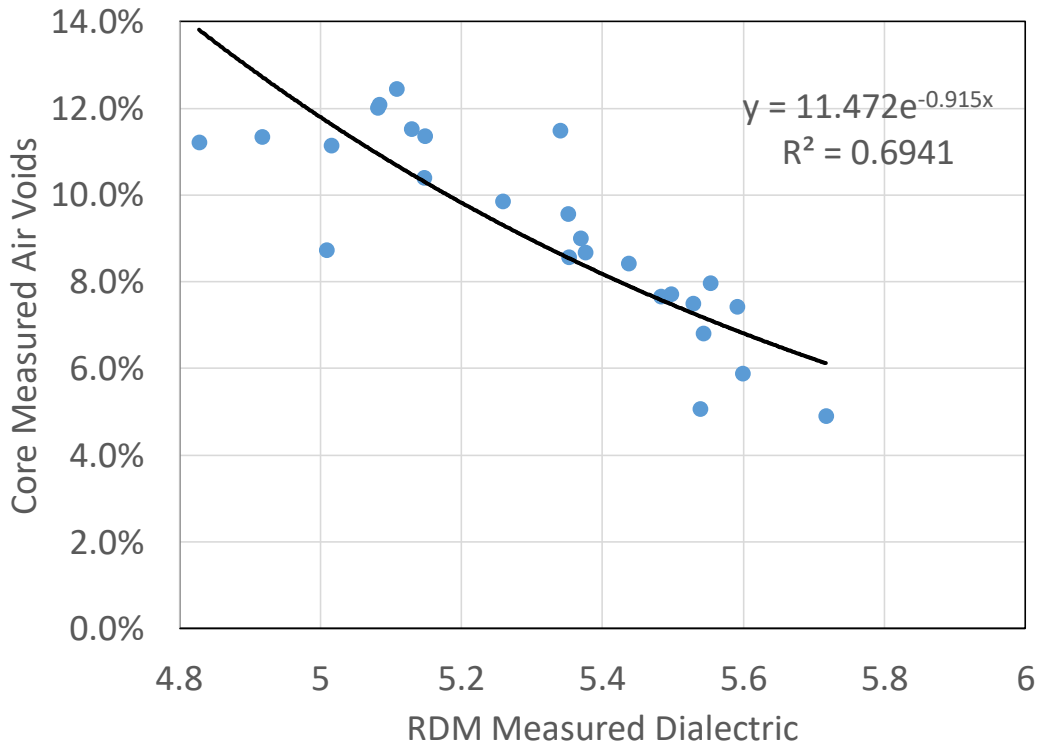


Figure 16. Correlation Model for All Wear Lifts

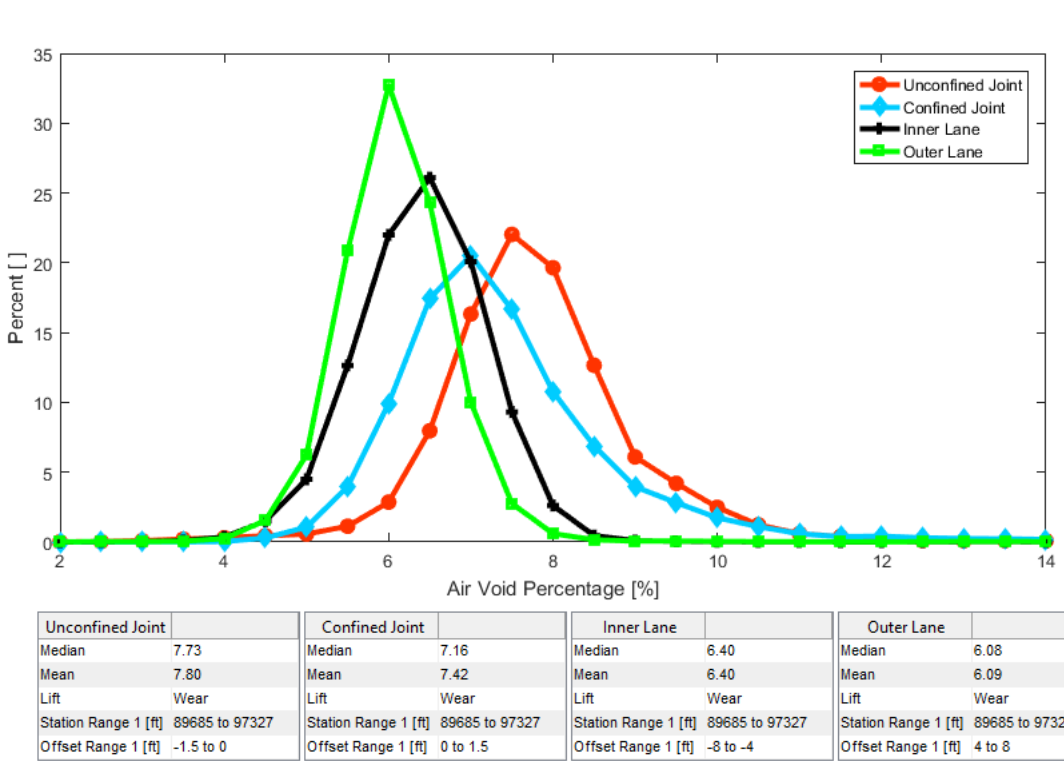
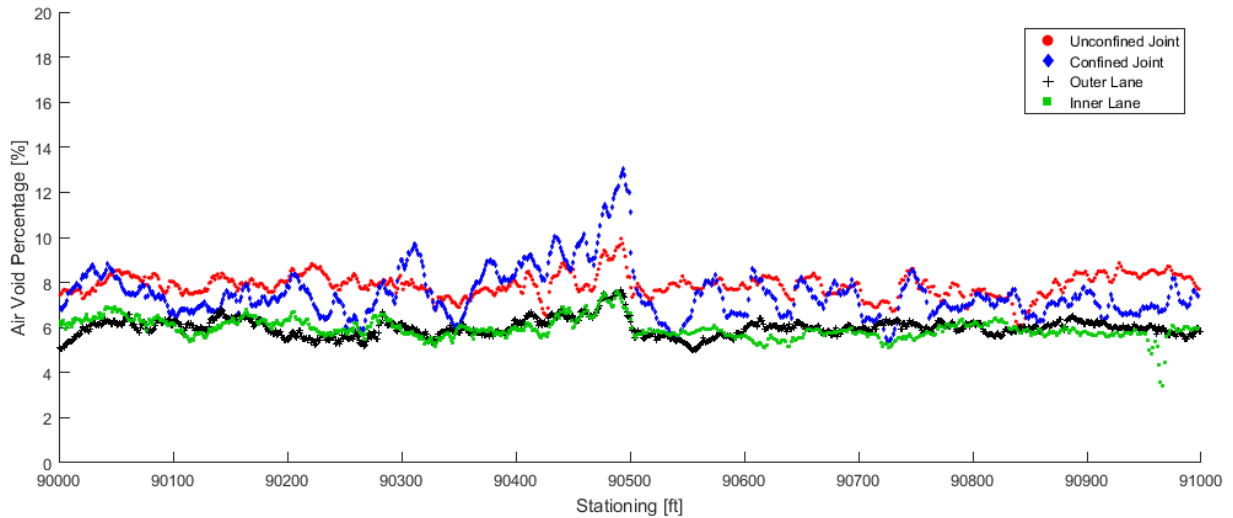


Figure 17. Frequency Distributions of Measured Air Void Content along HWY 52, Section 1



	Unconfined Joint		Confined Joint		Inner Lane		Outer Lane
Median	7.77	Median	7.09	Median	5.95	Median	5.89
Mean	7.90	Mean	7.57	Mean	6.00	Mean	6.00
Lift	Wear	Lift	Wear	Lift	Wear	Lift	Wear
Station Range 1 [ft]	90000 to 91000	Station Range 1 [ft]	90000 to 91000	Station Range 1 [ft]	90000 to 91000	Station Range 1 [ft]	90000 to 91000
Offset Range 1 [ft]	-1.5 to 0	Offset Range 1 [ft]	0 to 1.5	Offset Range 1 [ft]	-8 to -4	Offset Range 1 [ft]	4 to 8

**Figure 18. Variation of Measured Air Void Content, Section 1.**

Similar, Figure 18 shows consistently high air void content for the unconfined side of the joint. Although for some areas, air void content of the confined side of the joint was similar to that of the inner and outer lanes, and some locations was estimated to be as high as 12 percent.

#### 4.1.5.1.1 Comparison with Intelligent Compaction

In addition to the RDM testing, HWY 52 near Zumbrota, Minnesota was also used for evaluation of the Intelligent Compaction (IC) and IR technology. The IC was used to continually monitor compaction efforts during HMA paving operations. The IR was used to continually monitor the surface temperature of the mat immediately behind the paver screed during placement operations. This gave an opportunity to compare the data obtained from RDM, IC, and IR.

Figure 19 shows RDM-measured dielectric, IC-measured roller speed, and IR-measured HMA temperature after placing approximately 300-ft stretch of pavement, covering both lanes moving south from 1070+00 stationing. This stretch was selected since there were discrete differences in the RDM compaction results, which suggested there were some effects of changing construction operations or conditions. The following three distinct regions have been identified, as shown in Figure 19A:

1. Region 1 had the best compaction as indicated by higher dielectric readings (5.6 to 5.7).
2. Region 2 showed a sharp reduction in dielectric at the border with Region 1 and gradual increase in dielectric toward the southern end of the region.

3. Region 3 exhibited a high variability in the compaction level. While most dielectric reading varied between 5.2 and 5.4, some locations showed readings as high as 5.6 to 5.7.

Analysis of Figure 19B shows that the roller speed between 10 and 20 feet per minute (ft/min) for Region 2 was slightly lower than that of 30 ft/min for Region 1. However, the HMA mixture temperature during placement for Region 2 was much lower than for Region 1. While the HMA mixture pavement temperature for Region 1 varied between 275 degrees Fahrenheit (°F) and 299 °F, for Region 2 it was between 250°F and 274°F. It is important to note that in the southern portion of Region 2 where the temperature is higher, the compaction level is higher as well. This suggests that a drop in the pavement temperature during placement may lead to a lower compaction level, even if the speed of compaction is reduced. Region 3 shows a high variability in the HMA placement temperature, from 250°F to 300°F. In addition, the roller speed for Regions 3 was higher than for Regions 1 and 2, resulting a highly variable and mostly lower-compaction level.

It can be concluded that all three technologies, RDM, IC, and IR, provide valuable, complementing information that could be used for improvement of construction processes.

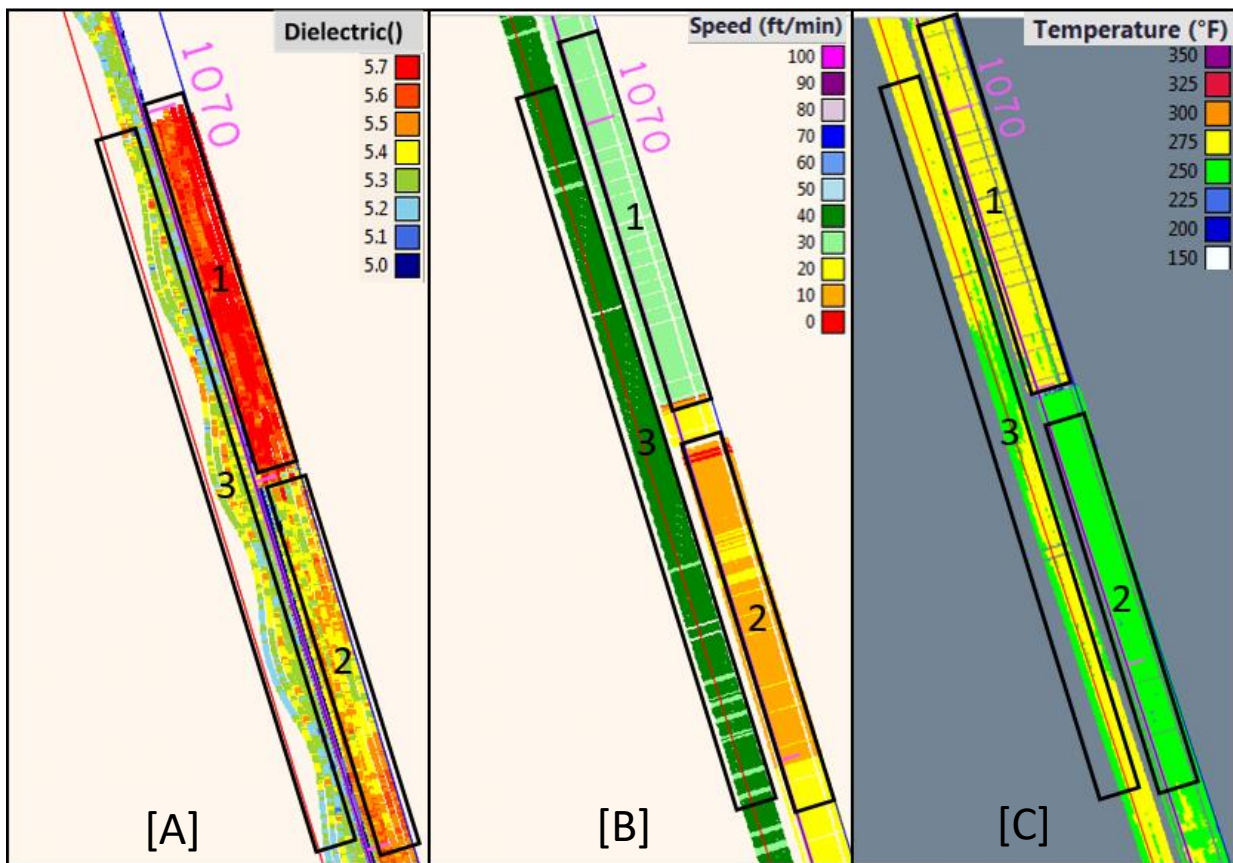


Figure 19. Dielectric, Temperature and Roller Speed [A] Rolling Density Meter Dielectrics, [B] Paver Speed, and [C] Infrared Scanner Measured Pavement Temperature

### 4.1.6 Conclusions

Nondestructive surveys of air voids were conducted on four sections of HWY 52 near Zumbrota, Minnesota, using the RDM device. Full-scale surveys covering miles of highway and producing millions of data points were conducted over the course of several weeks. The experience of the RDM survey crew was used to develop a recommended methodology for surveying new pavement in real time at a rate consistent with paving operations. The developed methodology focused on maximizing survey coverage of critical compaction regions and increasing the accuracy of the RDM and core data. Analysis of the GPR data was used to provide real-time feedback to paving crew, as well as to conduct post-project analysis of data. The data collected was used to evaluate overall achieved compaction, as well as to assess the effects of experimental construction practices.

## 4.2 U.S. Route 1 Cherryfield, Maine

The RDM survey was conducted on 1.25-inch overlay of U.S. Route 1 near Cherryfield, Maine on July 13, 2016. The total paving project extended from STA 10+00 to STA 219+05. It covered approximately 1,500 ft of pavement consisting of three non-consecutive 500-ft sections: the first one from STA 55+00 to STA 60+00, the second one from STA 75+00 to STA 80+00, and the final one from STA 93+00 to STA 98+00.

The RDM survey was the first trial survey conducted by the Maine DOT, and was predominately for training purposes. The sections were non-consecutive because the rate of RDM data collection was slower than the advancement of the paving operation. Therefore, the RDM survey team had to skip over sections to stay within the moving closure. Within the first two survey sections, RDM data was collected in both the center of the lane and along the longitudinal joint. The first two surveys were conducted with standard sensor offset, with the outer sensors offset 2 ft from the center sensors. The final survey was conducted as an experimental wheel path survey at the request of the Maine DOT and the offset was increased to the maximum, producing a distance of 5.5 ft between the outermost sensors.

A key part of this survey was the testing of new core data collection method developed based on lessons learned from the demonstration project near Zumbrota, Minnesota. The poor correlation between the RDM-measured dielectric constants and laboratory-measured air voids for one section were attributed to the lack of the RDM measurements taken directly at the core location. In this survey, once core locations were selected, the RDM cart was used to resurvey the section and determine the core location. The core locations were marked, and a small survey was performed over the core locations.

A total of five cores were collected. Two cores were collected within the first survey section and three cores were collected within the second survey section. High and low dielectric cores were selected with the first survey section, and high, low, and medium cores were selected within the

second section. The cores were marked by reviewing dielectric data after completion of a pass along a 500-ft section. The values were discussed, and, in general, the highest or lowest values were selected for coring. Core locations that exhibited a high variability in the dielectric values were rejected in favor of the core locations with more consistent values.

While more cores are generally desired, the cores did cover a large range of dielectric values and produced a good model. Figure 20 shows the results of calibration. An  $R^2$  of 0.93 was attained for the calibration. The calibration model appears to have a fairly consistent fit, providing good estimations for both high and low air void contents.

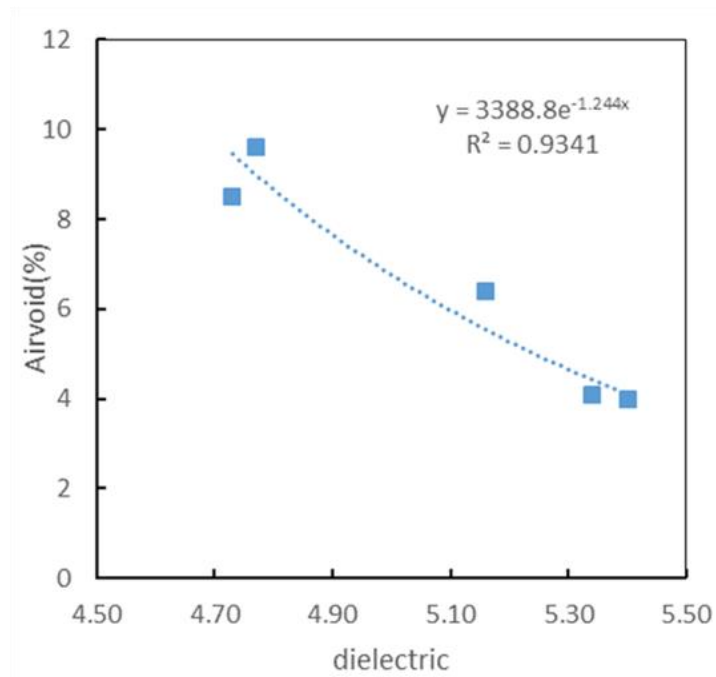


**Figure 20. Cherryfield, Maine Calibration Model**

The results of the survey were used for both real-time and post-construction investigations of achieved compaction. During the survey, the dielectric data collected were used to evaluate relative compaction. Large fluctuations in dielectric data collected within the center of the lane suggested inconsistent compaction. Discrete regions of very low dielectric were encountered, suggesting high air voids. For data taken along the joint, dielectric values suggested compaction was generally good, with occasional sections of low compaction. As this was the first trial implementation of the RDM technology by the Maine DOT, no action was taken based on the field data interpretation of the low dielectric regions.

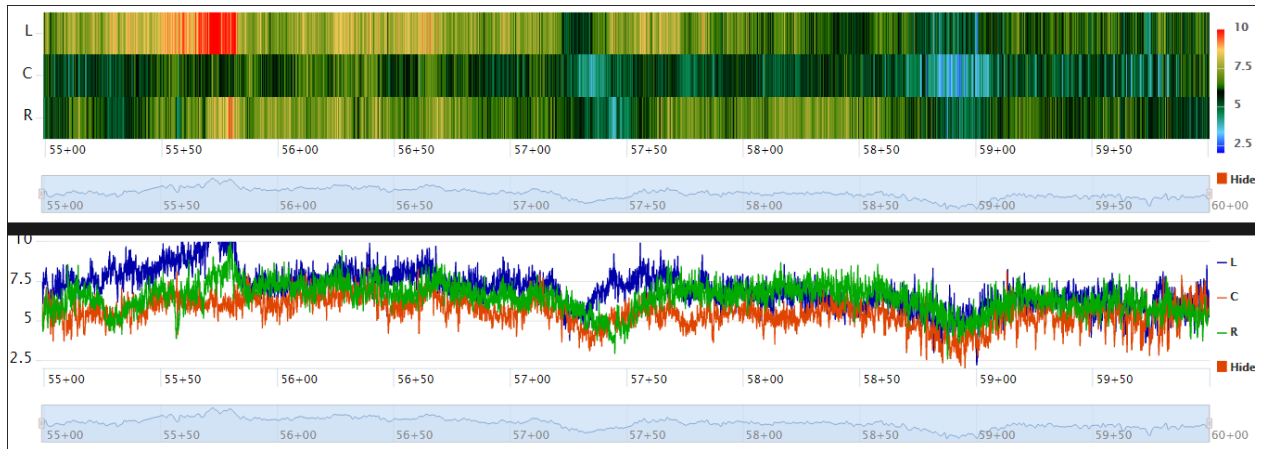
Conversion of the RDM survey dielectric data to air void data quantified the level of achieved compaction. The average air void content was around 6 percent, but both lane and joint data exhibited regions of very high air voids up to 14.6 percent. Figure 22 presents the resulting air voids heat maps and line graphs. The general statistics of the survey are presented in Table 11.

**Table 11. Cherryfield, Maine Basic Survey Statistics**

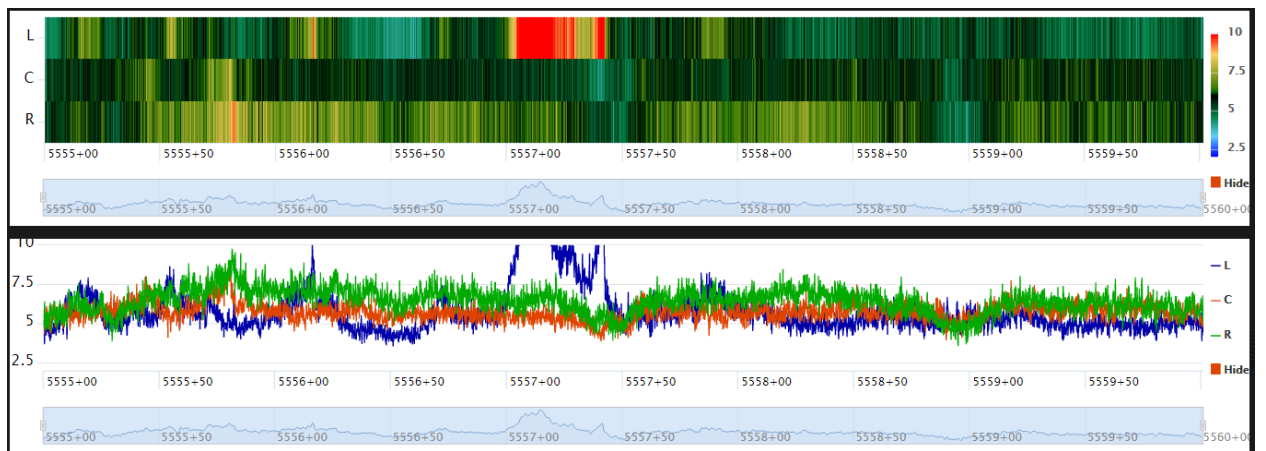
	Average	Maximum	Standard Deviation
Lane	6.22	14.60	1.11
Joint	6.32	18.63	1.12
Wheel Path	5.03	5.92	0.14

The center of the lane was found to consistently have the highest compaction and lowest variability of any data taken in the lane surveys. However, data recorded at the sensors offset 2 ft from the center reported lower and more variable compaction (Figure 22A and 21C). This report suggests a review of the centerline roller patterns may be needed. The lane data taken within the wheel path produced the best and the most consistent compaction compared to other datasets (Figure 22E). The average air voids were 1.2 percent lower than those reported for either the lane or the joint, and variability (as measured by the standard deviation) was nearly 1/10 of the variability observed in other datasets. It is important to note that this data set was taken 1,300 ft away from the next closest dataset and was also the only data taken in this section.

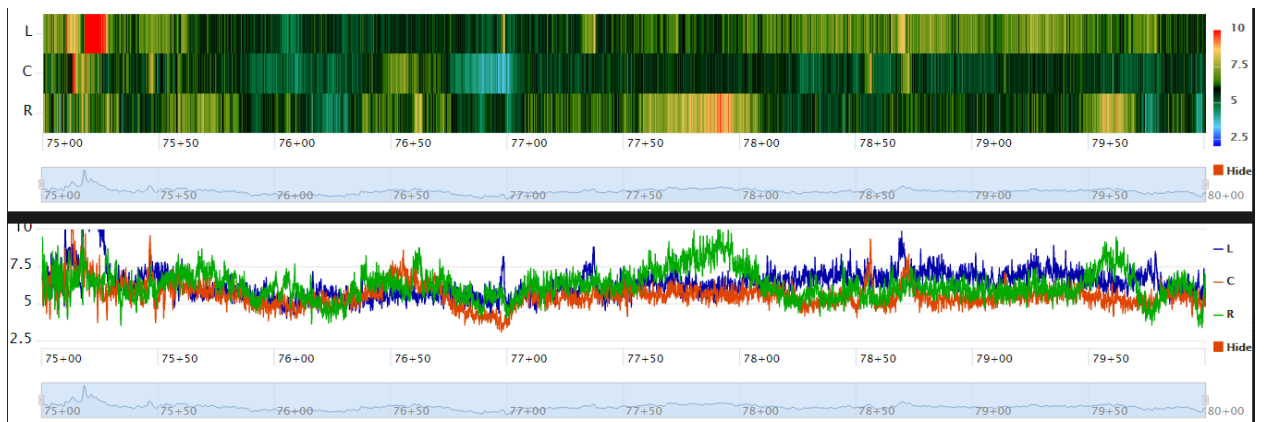
The good compaction results attained in the wheel path survey may be a function of the QA/quality control (QC) procedure currently used by Maine DOT that places a lot of emphasis on wheel path compaction, and the wheel path is the focus of much QA/QC testing. It is likely that contractor practices have been developed to reflect this focus, and that the current paving practices are optimized to achieve a good wheel path compaction. However, many studies have shown that compaction in other sections of the lane, especially along the joint, is as important for good pavement performance as compaction within the wheel path. Future implementation of the RDM in Maine should include the collection of lane, joint, and wheel path data within the same sections to get a better characterization of compaction across the lane. Like the lane survey data, the data taken along the joint indicated moderate and variable compaction. Average lane and joint compaction levels are similar, with joint compaction exhibiting a slightly higher average air void content. Generally, joint compaction can be expected to be significantly worse than lane compaction. There are several regions along the joint that exhibit very high air voids (greater than 10 percent) (Figure 22B and 21D). However, these regions are often discrete and do not cover a very long distance, suggesting that region was possibly missed by a roller; an issue that can easily be addressed.



A. Section 1 Lane Survey

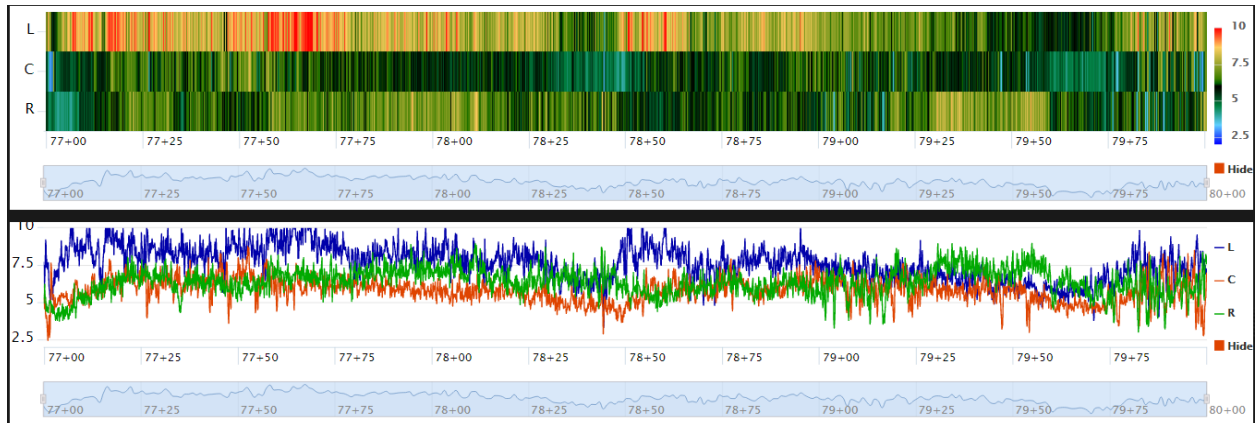


B. Section 1 Joint Survey

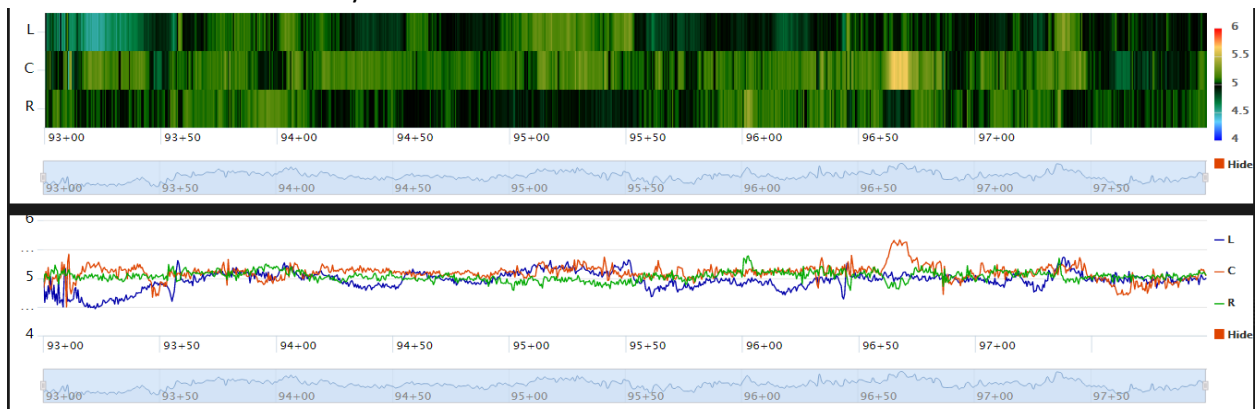


C. Section 2 Lane Survey

**Figure 21. U.S. Route 1 Air Voids Determined from Rolling Density Meter Survey**



D. Section 2 Joint Survey



E. Section 3 Wheel Path Survey

**Figure 22. U.S. Route 1 Air Voids Determined from Rolling Density Meter Survey (continued)**

The coverage of the survey was limited by the speed of the paving operation on a two-lane highway with a moving lane closure. In addition to the RDM survey training and implementation, the survey crew was also responsible for the collection of cores. All these issues resulted in the pace of RDM and core data collection being much slower than the advancement of the paving operation. To keep within the bounds of the closure, the survey data collection was rushed and the desired number of cores were not attained. The following are recommendations to avoid this rushed situation in future surveys:

- Implement RDM surveys on projects with full closures until more experience is gained.
- Ensure more personnel is available for core collection and RDM surveying.
- Conduct a survey with just one pass along only the most critical compaction region.
- Perform surveys without core data collection (real-time feedback on relative compaction can still be provided with dielectric data).

Finally, analysis of the air void versus dielectric calibration model suggests that collecting the RDM data directly over the core is crucial to achieving a good calibration model. This affirms the

hypothesis that a primary reason for the poor correlation seen in Zumbrota, Minnesota was the lack of measurements at the exact core location. These results suggest that even highly accurate GPS and distance encoders do not compensate for the exact core locations measurements.

### 4.3 HWY 2 near Lincoln, Nebraska

An RDM demonstration survey was conducted on July 19, 2016, on a 1.5-inch overlay of HWY 2 in Lincoln, Nebraska. As this survey was primarily a training exercise, significant efforts were focused on demonstration and explanation of the RDM and core data collection process to Nebraska DOT personnel. The RDM survey covered approximately 1,000 ft of pavement from STA 140+00 to STA 150+00 in two 500-ft long segments. RDM data were collected in both the center of the lane and along the longitudinal joint within the first segment, but only within the center of the lane along the second segment, as the battery was depleted.

The depletion of the batteries within the RDM device was not a result of any defect, but rather a result of a delay in the paving operation. Originally, paving was scheduled to begin around 8:00 pm. The RDM survey crew arrived onsite around 7:00 pm to begin early training and equipment warm up. However, the paving operation did not reach the survey area until around 12:00 am. During the intervening hours, the RDM device was being demonstrated and used on small trials. The battery then died around 3:00 am during the main survey. Therefore, the battery operated for nearly 8 hours, a time consistent with the RDM specifications.

The core locations were selected by reviewing dielectric data after completion of a pass along a 500-ft segment. The values were discussed, and, in general, the locations with the highest or lowest exhibited dielectric values were selected for coring. The exception to this was an anomalous low section encountered along the lane of the second 500-ft section survey. The low region resulted from a construction defect and it was decided that the compaction at this location was not representative of the rest of the project. Once core locations had been selected, the RDM cart was used to resurvey the section and mark the core location.

A total of eight cores were collected. Five cores were collected within the first 500-ft segment. Two high and one medium dielectric core were collected within the center of the lane of the first segment, and two low dielectric cores were collected near the longitudinal joint within the first segment. Three cores were collected within the second 500-ft segment at two high and one medium dielectric value locations within the center of the lane of the second segment. The collection of two low dielectric cores was intended for the longitudinal joint, but this collection was not possible due to battery depletion.

The results of the survey were used for both real-time and post-construction investigations of achieved compaction. During the survey, the dielectric data collected was used to make general estimations of the achieved uniformity of compaction. It was found that within the center of the lane, overall compaction was mostly uniform; however, areas of low dielectric were

encountered, suggesting poor compaction in those areas near the center of the lane. For data taken along the joint, dielectric values suggested compaction was generally good, with occasional segments of low compaction. Discrete regions of low dielectric encountered during the survey were identified and discussed. As this was the first trial implementation of the RDM technology by the Nebraska DOT, no action was taken based on the field data interpretation of the low dielectric regions.

Although more than eight cores are generally desired, the cores did cover a large range in dielectric values. The results of the core calibration are presented in Figure 23. An  $R^2$  of 0.825 was attained for the calibration. Conversion of the RDM survey dielectric data to air void data suggests that overall compaction was moderate, averaging around 6 percent air voids. Figure 24 presents the air void contents heat maps and line charts for both segments. It can be observed that both the lane and joint contain regions with high air void content. For example, a large spike in air voids was observed at 141+50 in the segment two-lane survey. This location was inspected and found to be an area of damaged HMA. It should be noted that the areas with high air void content are localized and represent only a small portion of the pavement area.

Interestingly, the center of lane consistently reported a higher air void content than the joint. Usually the center of the lane has higher compaction than edges of the lane. If lower compaction within the center of the lane is exhibited in future surveys in Nebraska, an investigation into the roller patterns is recommended to identify the compaction practice.

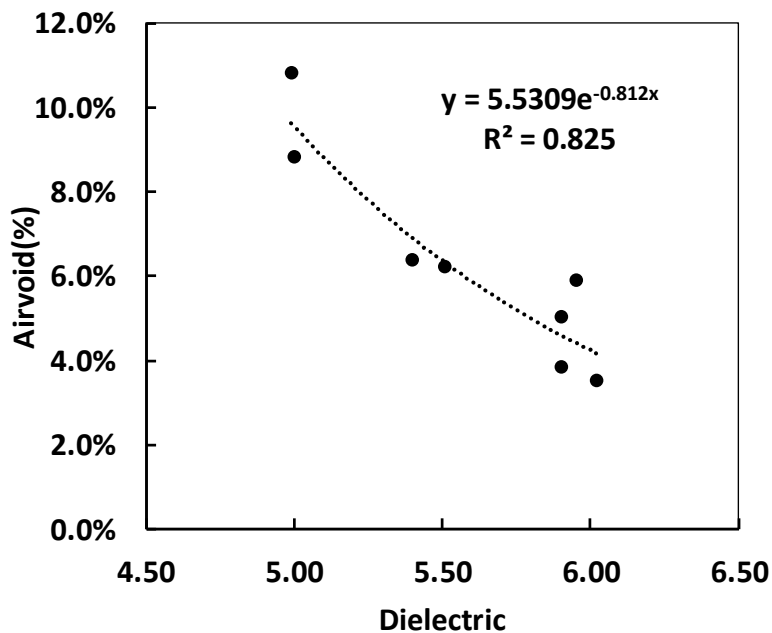
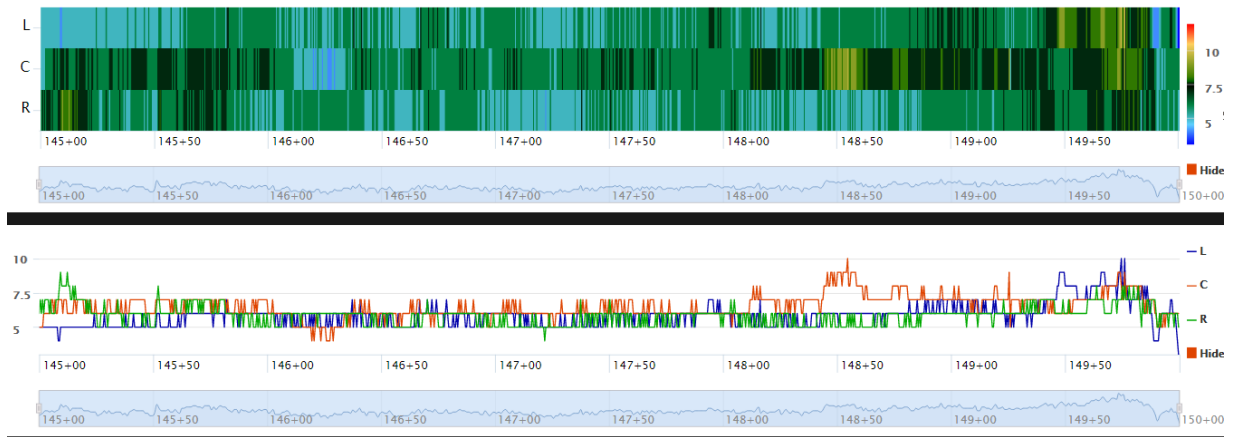
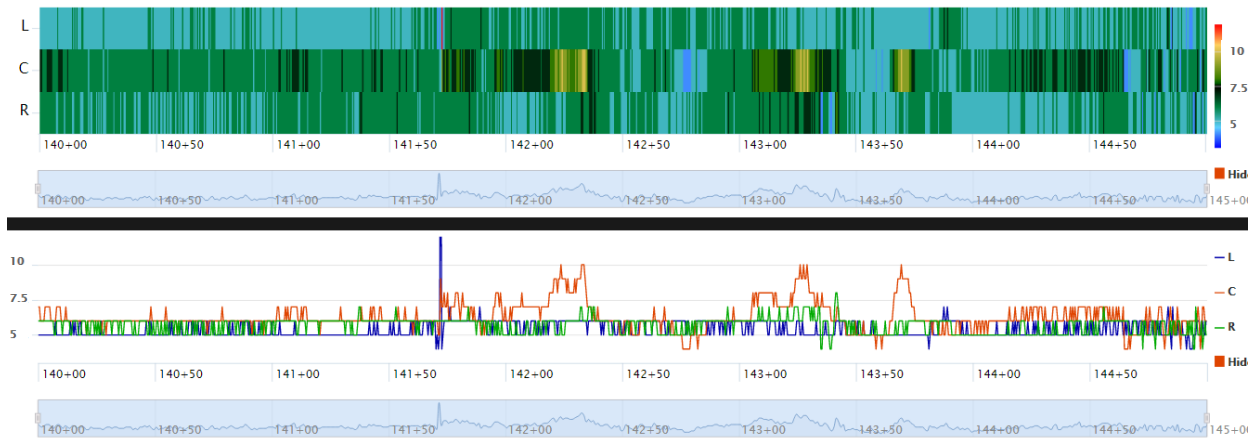


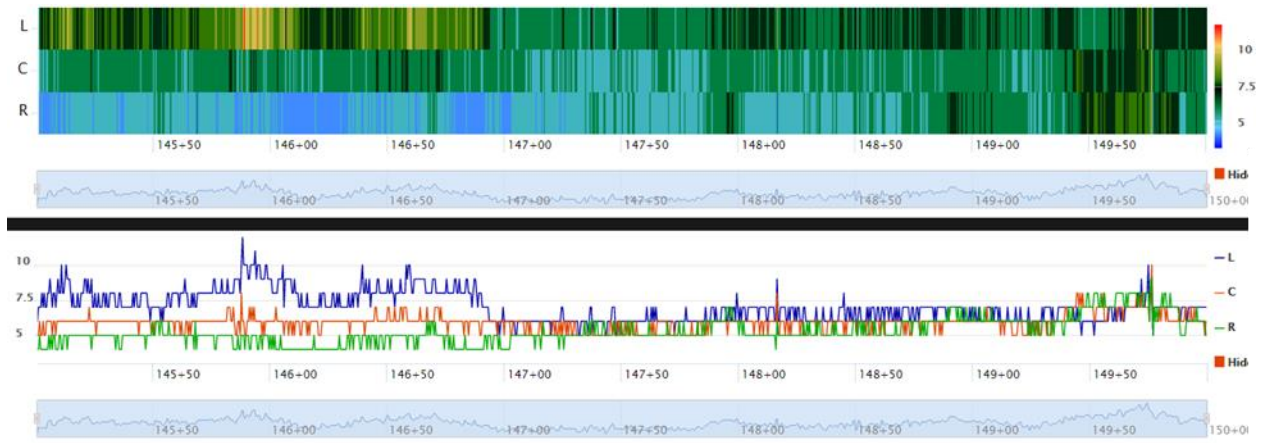
Figure 23. Lincoln, Nebraska Calibration Model



A. Segment 1 Lane Survey



B. Segment 1 Joint Survey



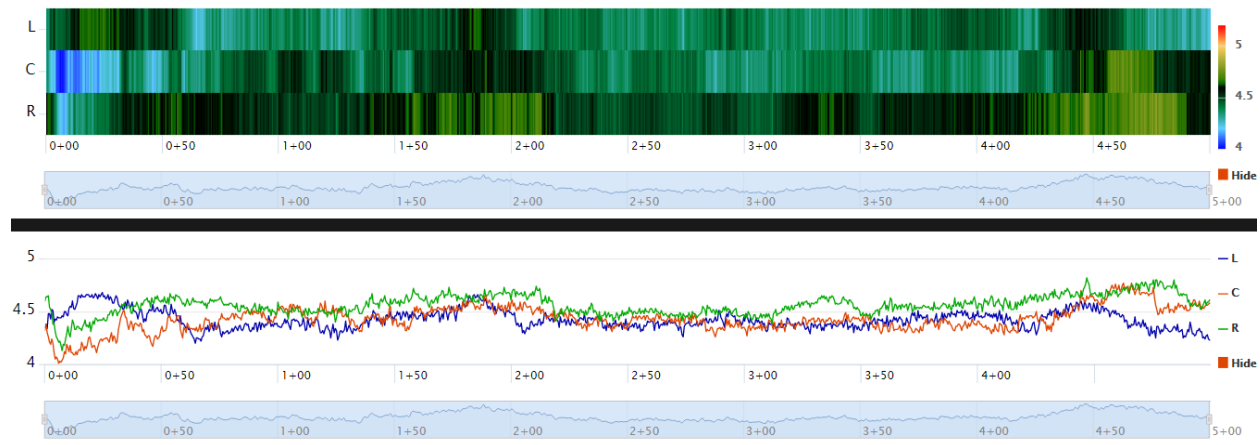
C. Segment 2 Lane Survey

Figure 24. Air Voids Content Heat Maps and Line Plots for HWY 2, Lincoln, Nebraska

## 4.4 HWY 9 near Clifton, Maine

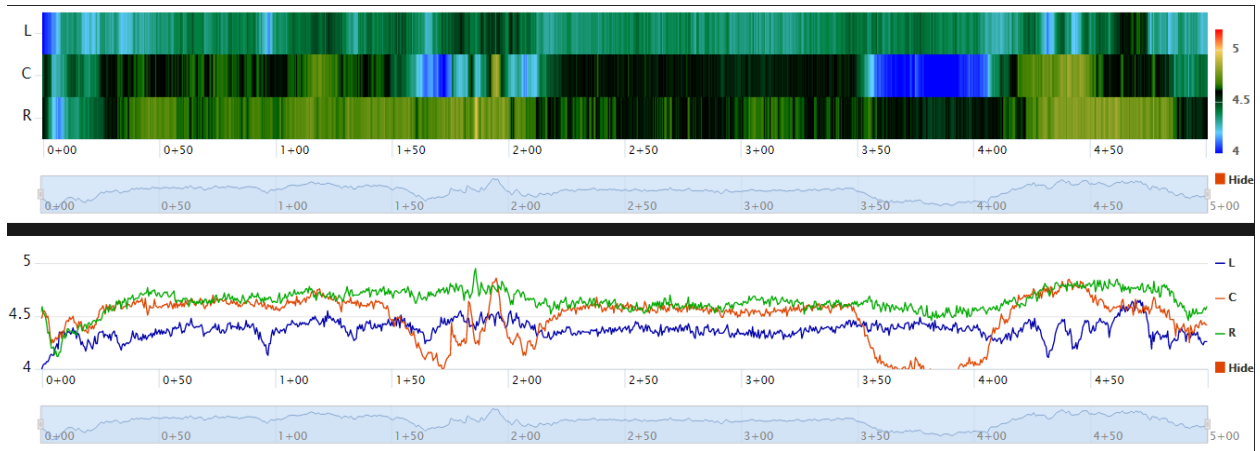
An RDM survey was conducted by Maine DOT personnel on September 19, 2016 on an HMA overlay of HWY 9 near Clifton in Maine. The data were collected on 1,500 ft of pavement length over three consecutive 500-ft segments of pavement. The first survey section was from STA 00+00 to STA 05+00, the second survey segment was from STA 5+00 to STA 10+00, and the final survey segment was from STA 10+00 to STA 15+00. Surveys were taken in both the shoulder and in the mainline over all sections. All the surveys were conducted with a wider than default sensor offset of 2.75 ft. This was done to maximize the coverage area of the survey and record data near both wheel paths in a single survey pass.

Figure 27 presents the results of the RDM measurements. During the surveys, the dielectric data collected were used to make a general assessment of the achieved compactions. The real-time survey data suggested that overall compaction was uniform, but the left sensor that was offset approximately 4 ft from the centerline longitudinal joint consistently reported a lower compaction. The dielectric values for the shoulder were similar to the values measured for the mainline. A few regions of low dielectric were noted; however, they rarely occurred and no action was taken.

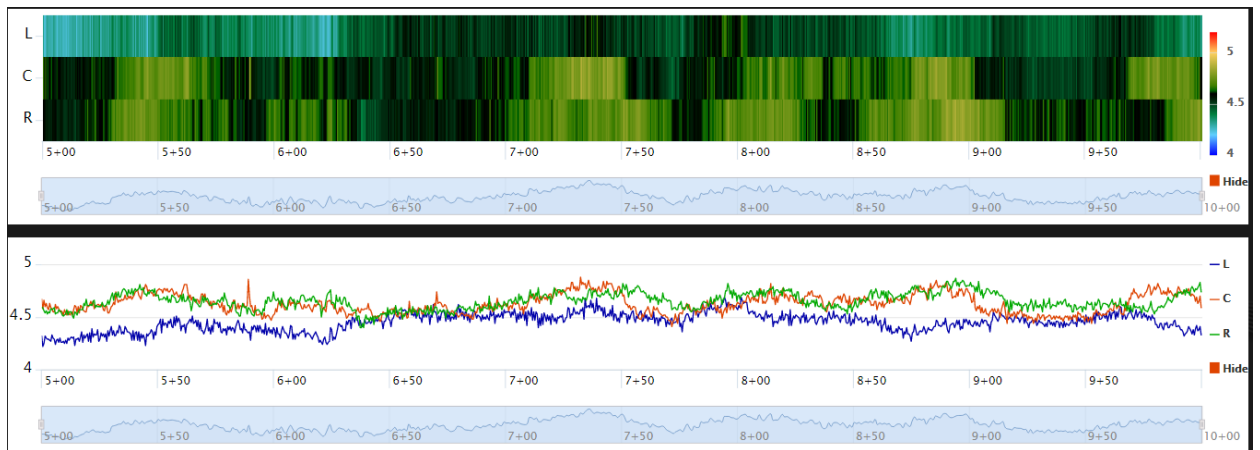


A. Segment 1 Lane

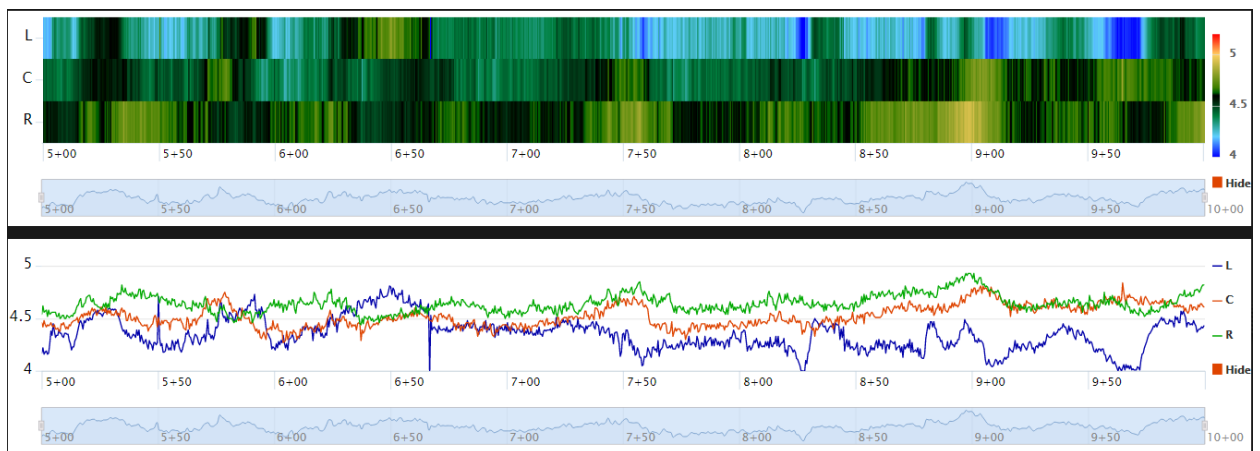
Figure 25. Heat Maps and Line Plots of Dielectric Data for HWY 9 near Clifton, Maine



**B. Segment 1 Shoulder**

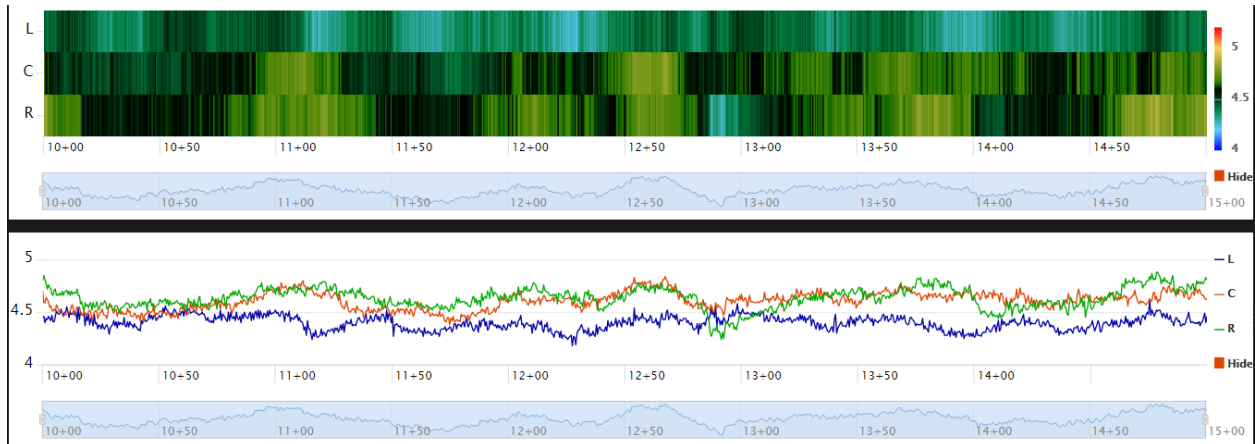


**C. Segment 2 Lane**

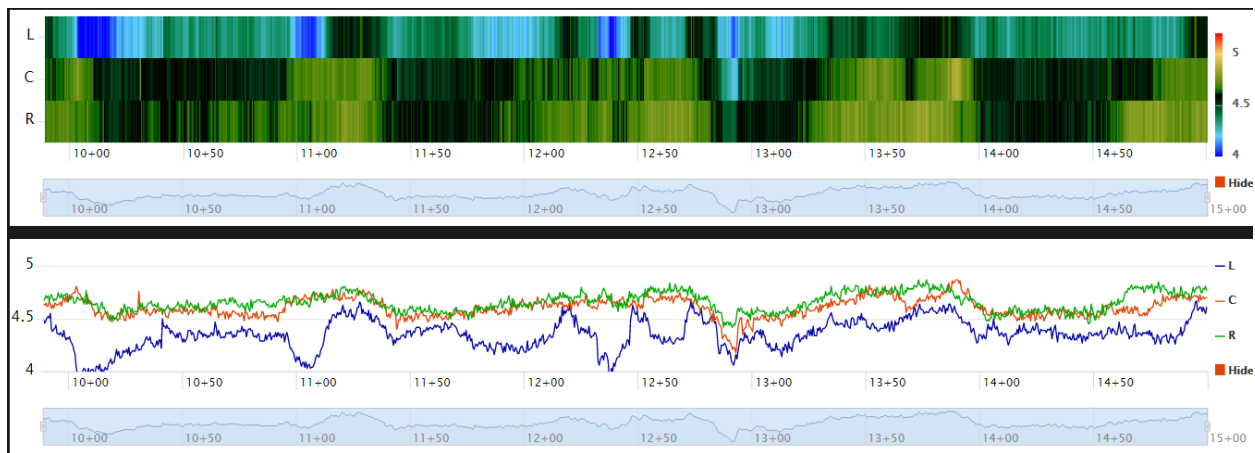


**D. Segment 2 Shoulder**

**Figure 26. Heat Maps and Line Plots of Dielectric Data for HWY 9 near Clifton, Maine (continued)**



E. Segment 3 Lane



F. Segment 3 Shoulder

**Figure 27. Heat Maps and Line Plots of Dielectric Data for HWY 9 near Clifton, Maine (continued)**

Because of time constraints, only four cores were collected for calibration purposes. Two cores were collected within high dielectric regions and two were collected within low dielectric regions. The cores were marked by reviewing dielectric data after completion of a pass along a 500-ft section. The values were evaluated and the regions with high or low values were selected for coring. Core locations that exhibited high variability in the dielectric were rejected in favor of the core locations with more consistent values. Once core locations had been selected, the RDM cart was used to resurvey the section and locate the core location. The resurvey procedure used at the core locations involved taking an approximately 2 ft distance-specified survey over the core location. This method records a dielectric every 0.1 ft and then outputs an averaged measurement for every 0.3 ft.

The laboratory-measured air voids for the cores were used to calibrate the air voids-dielectric model for this project. The results of the calibration are presented in Figure 28. An  $R^2$  of 0.56 was attained for the calibration. The calibration model appears to have a much better fit at low dielectric, high air void measurements than high dielectric, low air void measurements. The poor

fit is likely because of a small number of cores collected for this section, as well as a possible error in either dielectric properties or air void content for one of the cores with high measured dielectric constants. If more cores were collected for this section, the impact of a potential measurement error would not be as significant.

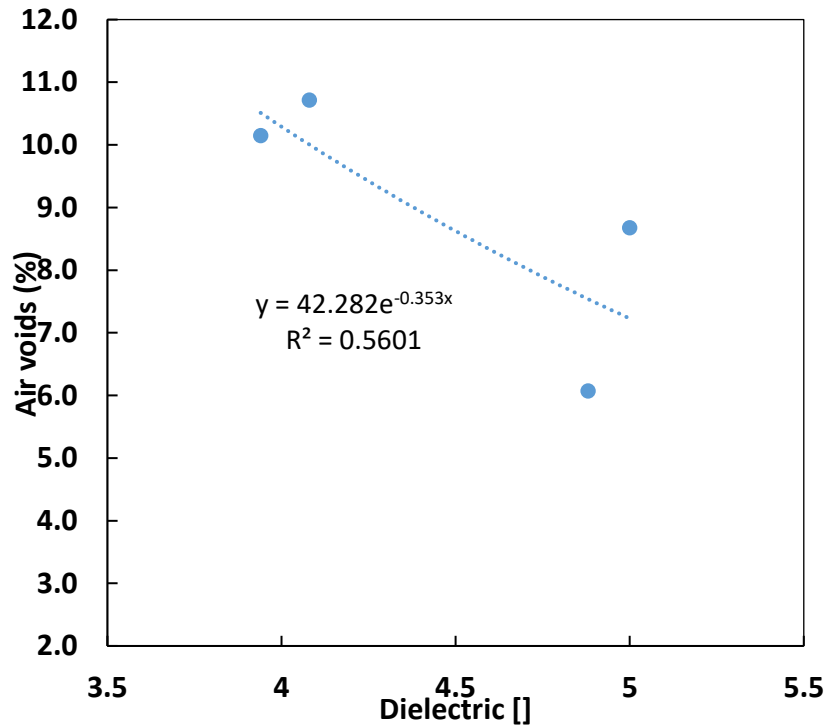


**Figure 28. Clifton, Maine Calibration Model**

Using the calibration curve, the measured dielectric values were converted into the air distribution. A summary statistics for the mainline and shoulder are provided in Table 12. Table 12 confirms the earlier observation that the compaction was quite uniform. However, the table suggests that the level of compaction was lower than desired, averaging around 8.5-percent air voids. The maximum offset shoulder survey performed approximately 15 ft from center of the lane reported the overall lowest compaction.

**Table 12. Clifton, ME Basic Survey Statistics**

	Offset <sup>a</sup> (ft)	Air Void Content		
		Mean	Minimum	Maximum
Lane	3.25	8.87%	7.60%	10.27%
	6	8.48%	7.15%	9.97%
	8.75	8.30%	7.06%	9.80%
Shoulder	14.75	8.20%	7.09%	9.73%
	12	8.53%	7.13%	10.23%
	9.25	9.09%	7.02%	13.49%

Note:

a. Measured from the longitudinal joint.

## 4.5 I-95 Near Pittsfield, Maine

An RDM survey was conducted by Maine DOT personnel on an overlay project of I-95 near Pittsfield, Maine on October 3, 2016. The survey was conducted in the south-bound direction on the final wear pavement lift over a 2,000-ft-long pavement section. The data was collected over four consecutive 500-ft segments. The first survey segment was from STA 1868+00 to STA 1863+00, the second survey segment was from STA 1861+00 to STA 1856+00, the third survey segment was from STA 1856+00 to 1851+00, and the final survey segment was from STA 1851+00 to STA 1846+00.

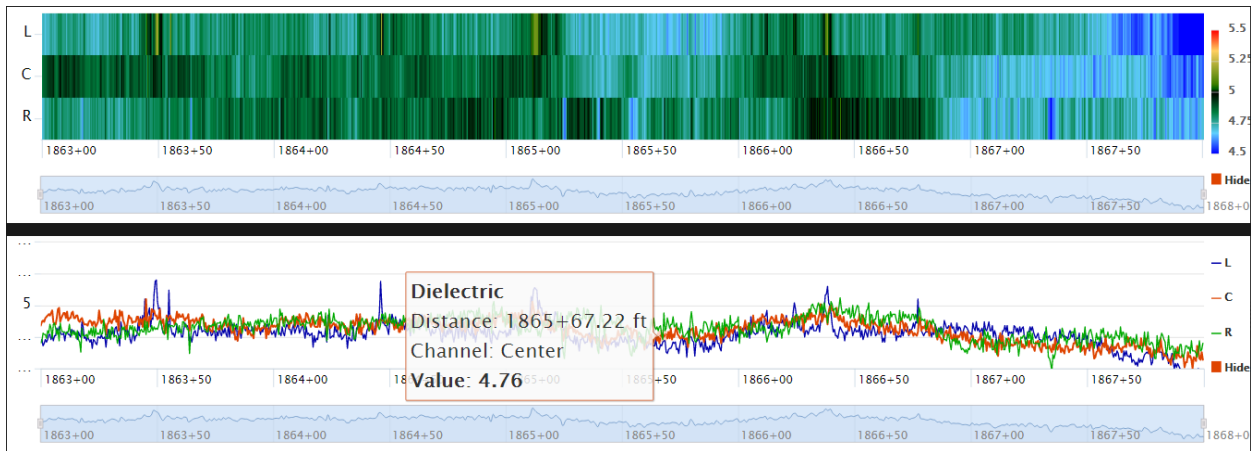
Surveys were taken both near the joint and in the mainline over all segments. All the surveys were conducted with a wider than default sensor offset of 2.75 ft. The mainline survey had the central RDM antenna path positioned 6 ft away from the longitudinal joints, that is, at the center of the lane. The left and right antenna paths were 3.25 ft away from the longitudinal joint and the shoulder joint, respectively. The longitudinal testing survey had the left antenna positioned 1.25 ft away from the longitudinal joint; the center and right antennas were located 4 and 6.75 ft away from the longitudinal joint, respectively.

The dielectric data collected was used to make a preliminary evaluation of the achieved compactions.

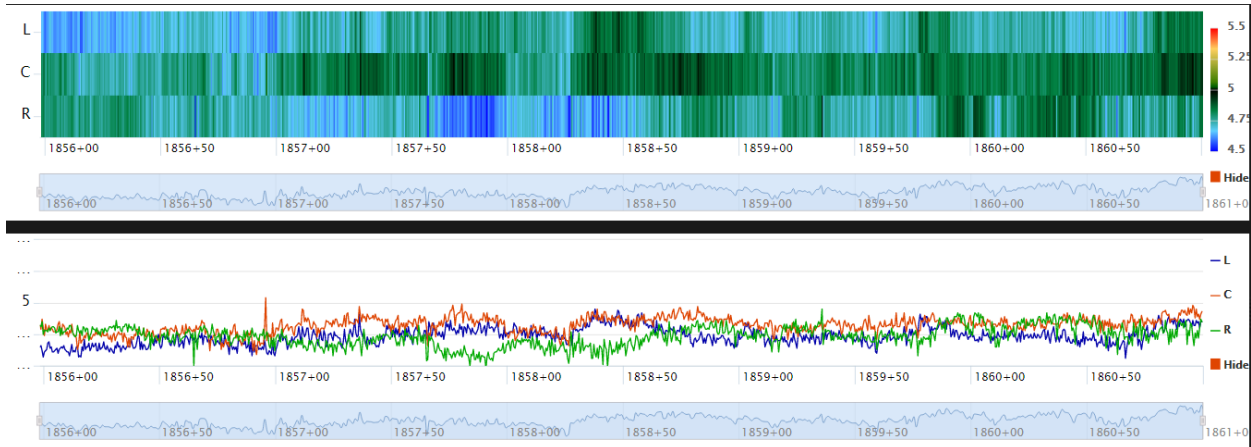
Figure 30 presents the dielectric maps for segments 1 through 4 measured at the center of the lane. Overall, the dielectric values and, correspondingly, compaction, were consistent. The exceptions are an area at the end of segment 1, beginning of segment 2, and the end of segment 3, which exhibited a lower dielectric constant corresponding to a higher air voids content. Figure 32 presents the dielectric maps for segments 1 through 4 measured near the longitudinal joint. The measurements 1.25 ft away from longitudinal joint resulted in consistently

lower dielectric values indicating a higher air void content near the joint. This measurement result is not surprising, as compaction is often lower near the joint.

A total of six cores were collected: three within high dielectric regions, two within moderate dielectric regions, and one within a low dielectric region. The cores were marked by reviewing dielectric data after completion of a pass along a 500-ft segment and, in general, the highest or lowest values were selected for coring. Core locations that exhibited high variability in the dielectric were rejected in favor of the core locations with more consistent values. Once core locations had been selected, the RDM cart was used to resurvey the segment and identify the core location.

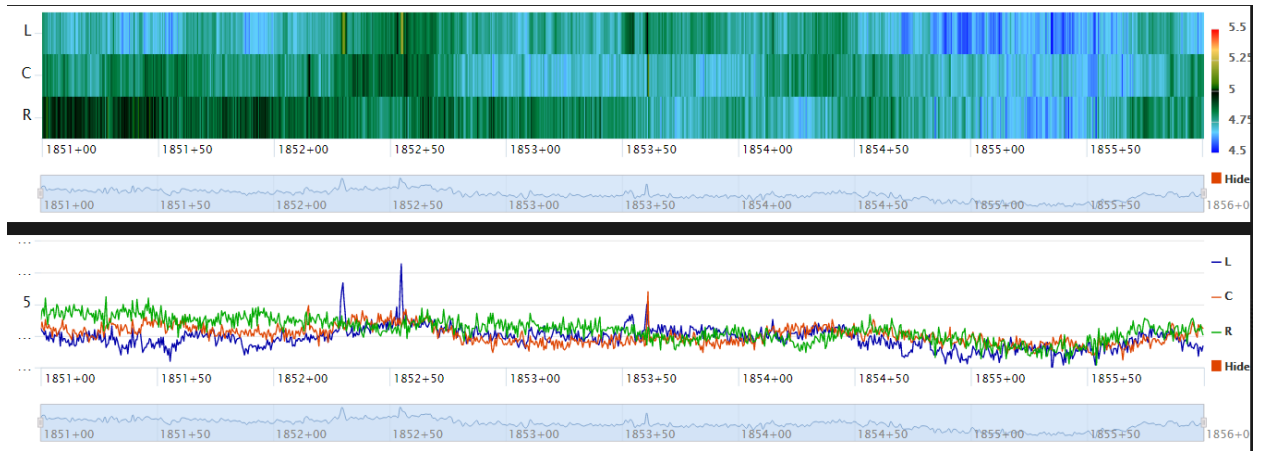


A. Segment 1

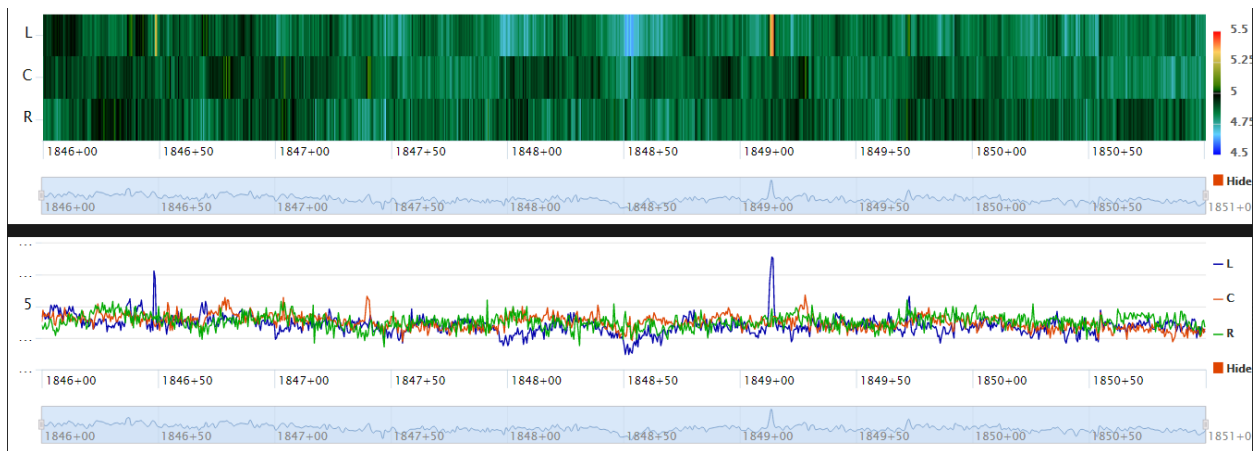


B. Segment 2

**Figure 29. Dielectric Maps from Joint Surveys of I-95 near Pittsfield, Maine**

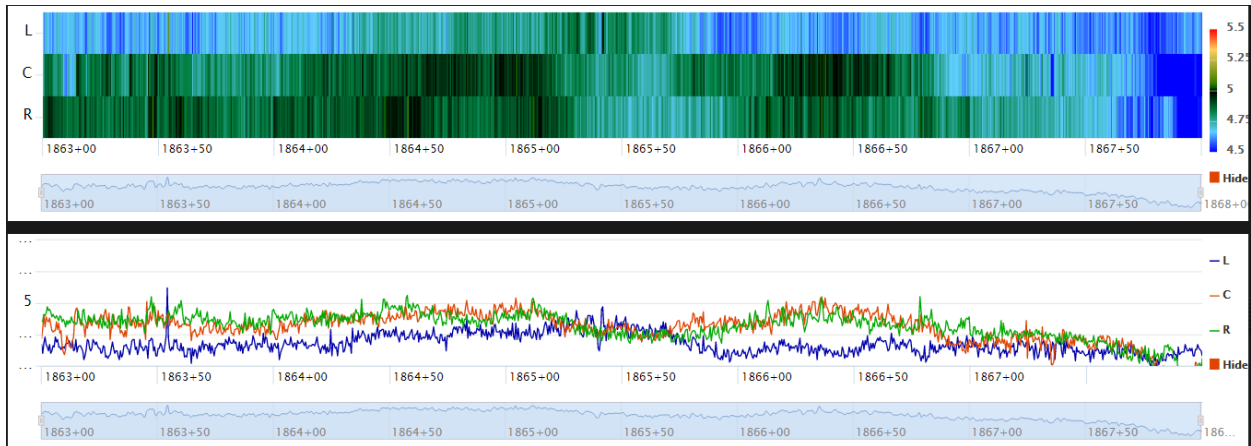


C. Segment 3

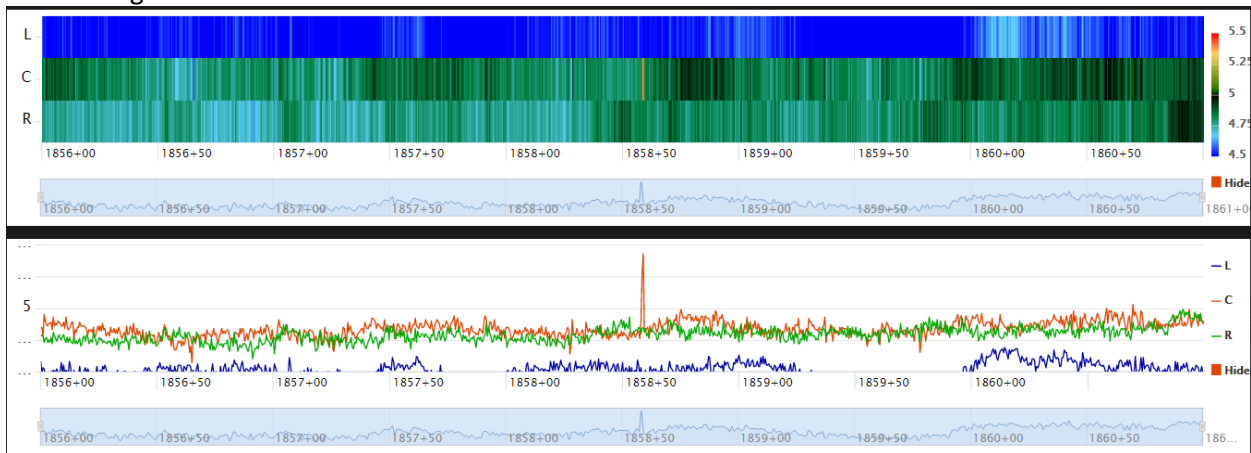


D. Segment 4

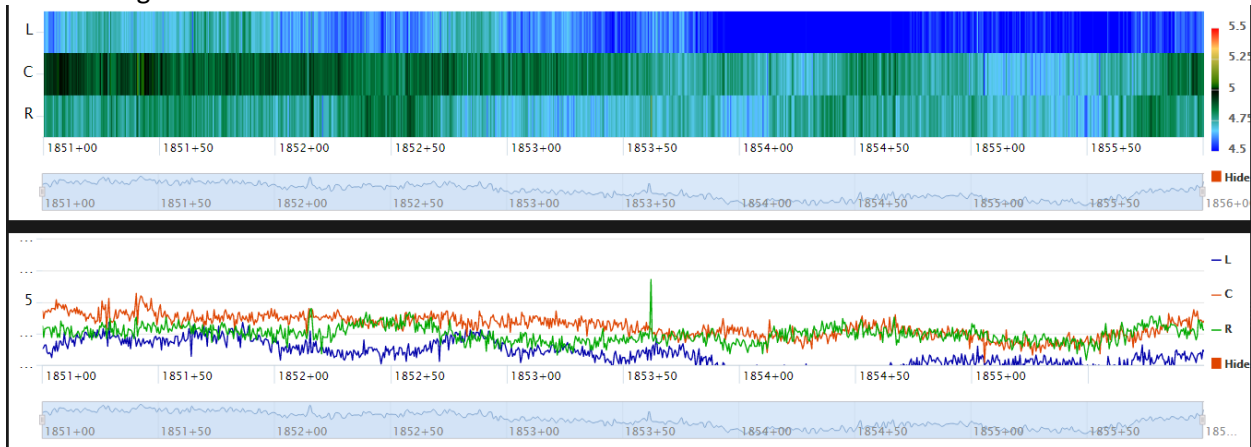
**Figure 30. Dielectric Maps from Joint Surveys of I-95 near Pittsfield, Maine (continued)**



A. Segment 1

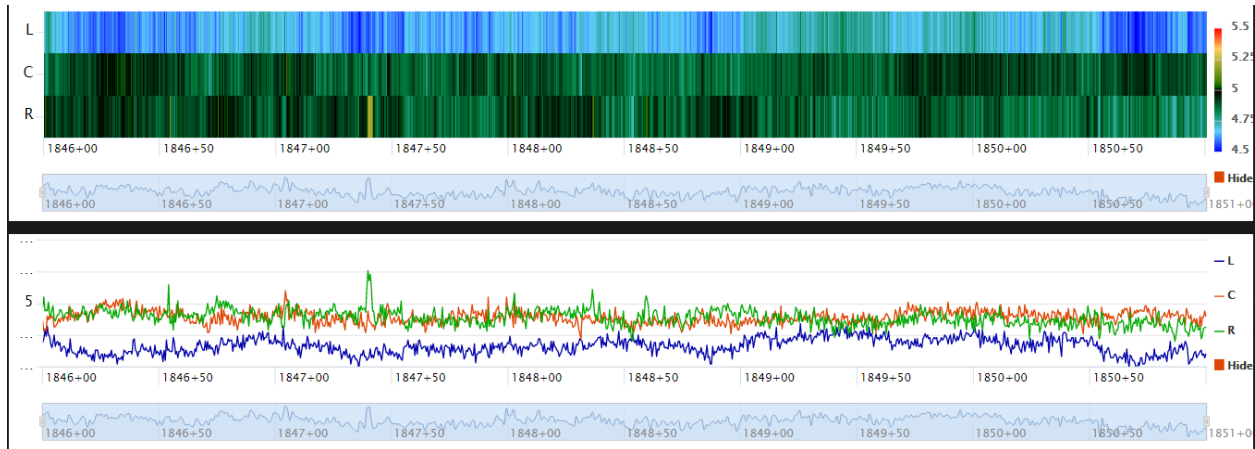


B. Segment 2



C. Segment 3

**Figure 31. Dielectric Maps from Joint Surveys of I-95 near Pittsfield, Maine**



D. Segment 4

**Figure 32. Dielectric Maps from Joint Surveys of I-95 near Pittsfield, Maine (continued)**

The resurvey procedure used at the core locations involved taking an approximately 2 ft distance-specified survey over the core location. This method records a dielectric every 0.1 ft and then outputs an averaged measurement for every 0.3 ft. This procedure is not recommended and was discontinued in favor of the time-specified method. The results of the core calibration are presented on Figure 33). An  $R^2$  of 0.62 was attained for the calibration.

Conversion of the RDM survey dielectric data to air void data suggests that overall compaction was good, averaging around 6 percent air voids. Table 13 presents basic statistics for each segment and antenna measurement. Both lane and joint data generally exhibited uniform compaction, with the exception of a lower compaction observed at the left sensor during the joint surveys (1.25-ft offset). It is also important to note that the results from the RDM measurement with the central antenna from the lane pass and the right antenna from the joint survey are similar, indicating a lack of bias in measurements with two RDM antennas.

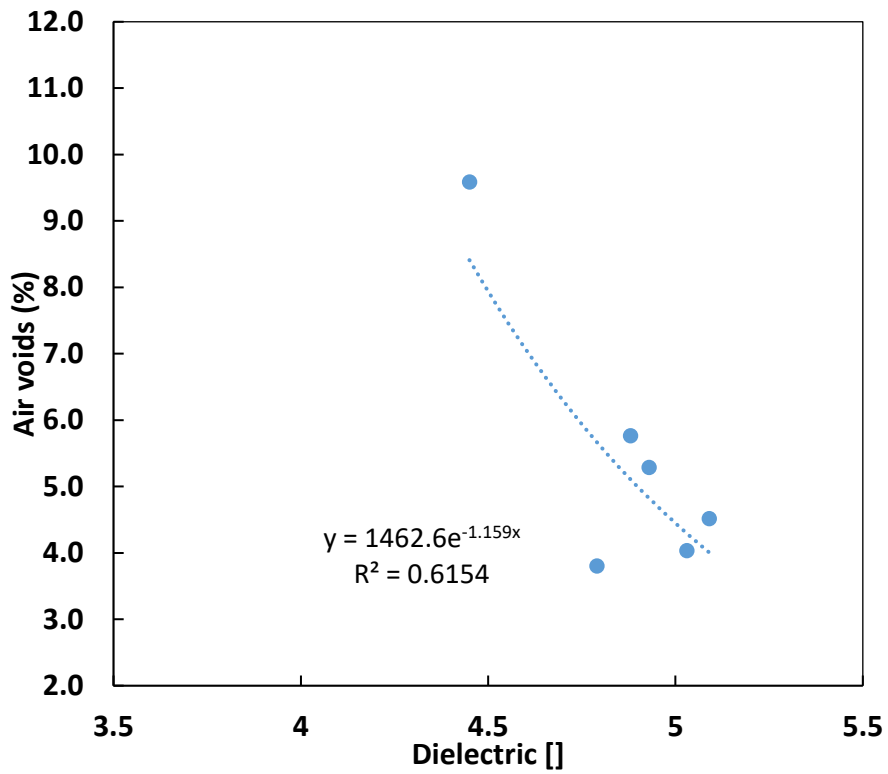


Figure 33. Pittsfield, Maine Calibration Model

Table 13. Pittsfield, Maine Basic Survey Statistics

	Offset (ft)	Mean	Minimum	Maximum
Lane Data	3.25	5.55	2.24	9.18
	6	5.26	2.79	8.26
	8.75	5.32	3.04	9.09
Joint Data	1.25	6.83	3.79	11.18
	4	5.14	2.70	9.30
	6.75	5.30	2.73	8.91

## 4.6 HWY 14 near Eyota, Minnesota

The RDM surveys were conducted from August 30, 2016 to September 12, 2016, on a 1.5-inch overlay of HWY 14 near Eyota, Minnesota. The surveys covered approximately 12 miles of road, beginning at STA 370+00 and continuing to the end of the paving at STA 411+50. Only the top-most lift of pavement was analyzed during the surveys. Multiple passes on certain sections, surveying both lanes, and the use of three sensors resulted in nearly 130 miles of data being collected. The primary goal of the HWY 14 demonstration project was to test the modifications in the test protocol developed based on the experience accumulated from the RDM demonstration project on the HWY 52 near Zumbrota, Minnesota, as well as the demonstration projects in Nebraska and Maine. In this project, a more rigorous core data collection methodology aimed to improve the accuracy of GPR estimated air voids was implemented.

MnDOT divided the project into six sections that were differed by the mix design or number of roller passes:

- Section 1 consisted of HMA constructed using standard construction practices, considered a control scenario. Three passes of the final cold roller were used. The mix had a maximum aggregate size of 3/4 inch. Approximately 66 miles of RDM data were collected for Section 1.
- Section 2 used the exact same mix design as Section 1, but an additional roller was used for compaction, for a total of four rollers. Approximately 12 miles of RDM data were collected for Section 2.
- Section 3 used three rollers, but the aggregate in the HMA mix was changed so that the maximum aggregate size was 1/2 inch. Approximately 7 miles of RDM data were collected for Section 3.
- Section 4 used four rollers in the same configuration as section two, with a maximum aggregate size of 0.5 inch. Approximately 8 miles of RDM data were collected for Section 4.
- Section 5 used a mix with 0.5-inch maximum aggregate, with the addition of Evotherm, the mix additive. Three rollers were used for this section. Approximately 21 miles of RDM data were collected for Section 5.
- Section 6 used the same mix design as the first section, but with the addition of Evotherm to the mix. Approximately 13 miles of RDM data were collected for Section 6.

A total of 30 cores were collected for calibration of dielectric to air void conversions. Locations with dielectric readings ranging from high to low were selected and marked for coring. For each marked location, hundreds of static time-specified measurements over the immediate core location and dynamic time-based measurements within a 6-inch vicinity of the core location were made. Both the static and dynamic surveys were conducted over 10 to 20 seconds with 10 measurements recorded per second, resulting in hundreds of dielectric constant

measurements of the location and of the surrounding area. The median dielectric constant values were then calculated for each location.

MnDOT’s standard laboratory procedure incorporating the American Association of State Highway and Transportation Officials (AASHTO) T166 test method for determining air voids was used for each core. These air void contents were then compared with the RDM dielectric readings taken for each core location. These comparisons were used to create core calibration models relating dielectric reading to air void content. The core calibration model for the entire paving project is shown on Figure 34. Laboratory measured air void values were correlated with RDM-surveyed dielectric values to produce models relating dielectric to air voids.

The collected cores with location, project, RDM dielectric and measured air voids are summarized in Table 14. Although air voids were calculated using both AASHTO T166 method and Corelok, the models were created using the T166 determined methods, as this is methodology commonly used by state agencies. However, when core data were filtered, comparison of the T166 and Corelok was used to identify possible outliers. The calibration model using all cores produced a reasonable fit, with an R<sup>2</sup> value of 0.7423. Although the fit obtained using the core data form all sections is quite good, much better fits were obtained for individual sections. Because of limited numbers of cores for Sections 3 through 6, Sections 3 and 4 and Sections 5 and 6 were grouped. Figure 35 shows the obtained calibration models, which shows that the coefficients of determination for each of these regressions are greater than 0.8.

**Table 14. Total Core Summary for Eyota, Minnesota Project**

Core ID	Date Paved	Core Station	Section	Direction	Offset (ft)	Corelok Air Voids (%)	T166 Air Voids (%)	Dynamic Dielectric
14Cal01	9/1/16	9965.4	1	EB	6	4.62	4.93	5.46
14Cal02	9/1/16	9735.9	1	EB	6	5.53	5.56	5.35
14Cal03	9/1/16	10474	1	EB	2.5	8.25	8.35	5.08
14Cal04	9/1/16	10474	1	EB	0.5	7.80	7.72	5.10
14Cal05	9/1/16	10751	1	EB	6	6.87	6.83	5.20
14Cal06	9/1/16	12030.7	1	EB	2.5	8.31	8.40	5.05
14Cal07	9/1/16	12030.7	1	EB	0.5	7.24	7.01	5.09
14Cal08	9/1/16	12029	1	EB	6	6.85	6.87	5.16
14Cal09	9/1/16	15300	1	EB	6	7.85	7.45	5.31
14Cal10	9/1/16	15300	1	EB	8	7.61	7.67	5.14
14Cal11	9/1/16	16191	1	EB	6	4.90	5.00	5.59
14Cal12	9/1/16	10497	2	WB	-6	6.50	6.61	5.40
14Cal13	9/1/16	10522	2	WB	-0.5	7.31	7.36	5.17

**Table 14. Total Core Summary for Eyota, Minnesota Project**

Core ID	Date Paved	Core Station	Section	Direction	Offset (ft)	Corelok Air Voids (%)	T166 Air Voids (%)	Dynamic Dielectric
14Cal14	9/1/16	11679	2	WB	-4	5.34	5.71	5.58
14Cal15	9/1/16	16473	2	WB	-4	6.03	6.10	5.45
14Cal16	9/1/16	16473	2	WB	-8	6.09	5.88	5.52
14Cal17	9/6/16	28364	3	EB	8	8.53	9.06	5.06
14Cal18	9/6/16	28405	3	EB	8	6.16	6.24	5.44
14Cal19	9/6/16	24374	4	WB	-6	3.85	4.44	5.50
14Cal20	9/6/16	24525	4	WB	-2.25	6.42	6.39	5.24
14Cal21	9/6/16	26704	4	WB	-6	4.91	5.43	5.40
14Cal22A	9/6/16	26752	4	WB	-6	4.64	4.47	5.49
14Cal23	9/6/16	26877	4	WB	-2.25	5.59	5.73	5.30
14Cal24A	9/6/16	26698	4	WB	-0.25	7.25	7.60	5.17
14Cal25	9/8/16	37990	5	EB	8	6.28	6.59	5.25
14Cal26	9/8/16	38065	5	EB	6	5.37	5.30	5.35
14Cal27	9/8/16	38105	5	EB	6	7.60	7.80	4.94
14Cal28	9/8/16	34161	5	EB	6	8.40	8.28	4.98
14Cal29	9/8/16	32787	6	WB	-0.25	9.98	9.44	4.92
14Cal30A	9/8/16	36196	6	WB	-6	8.67	8.50	4.76

Notes:

EB = eastbound

WB = westbound

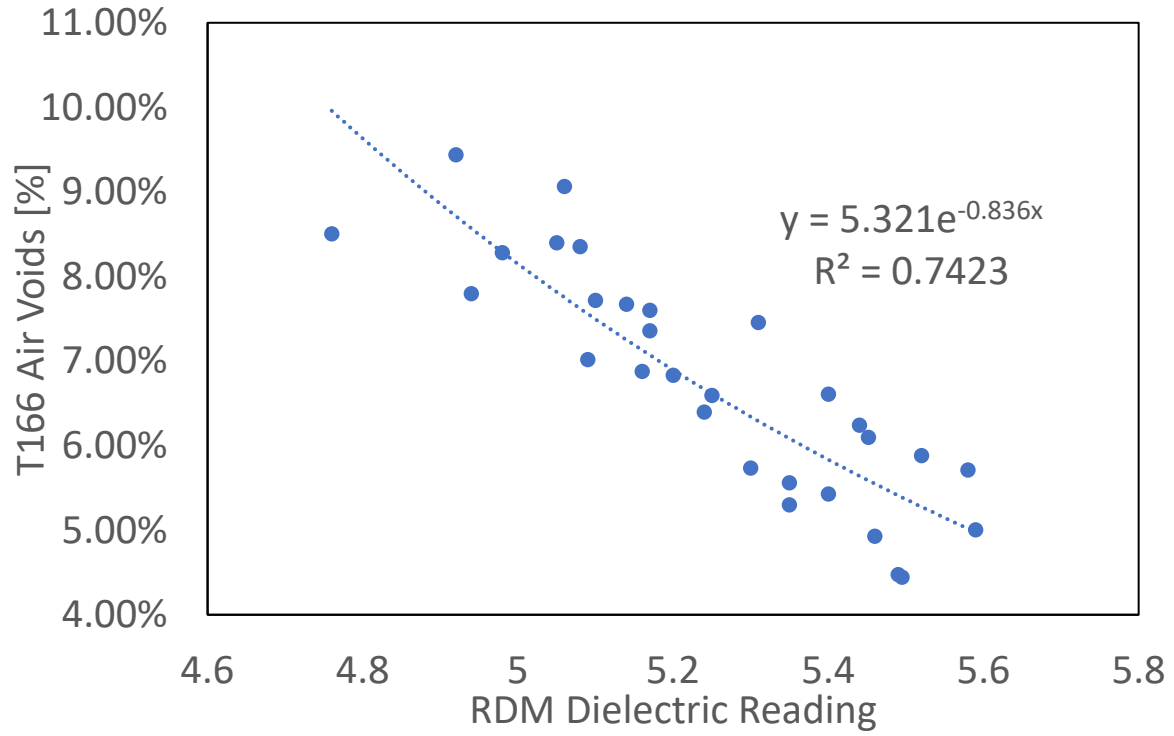
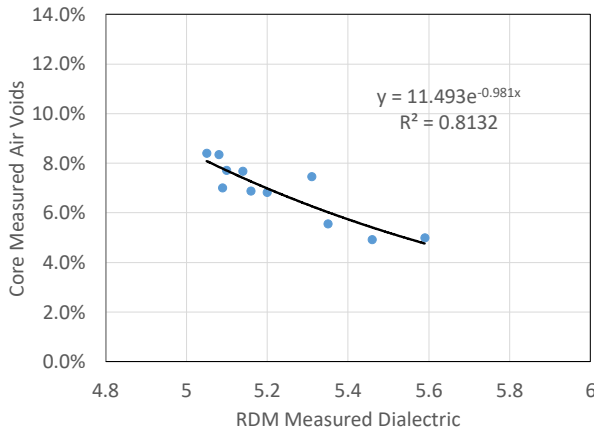
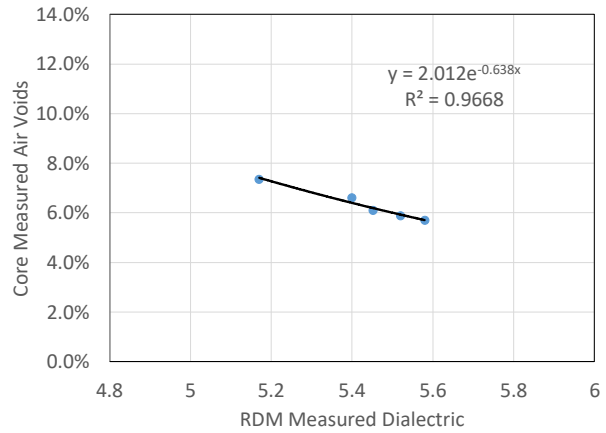


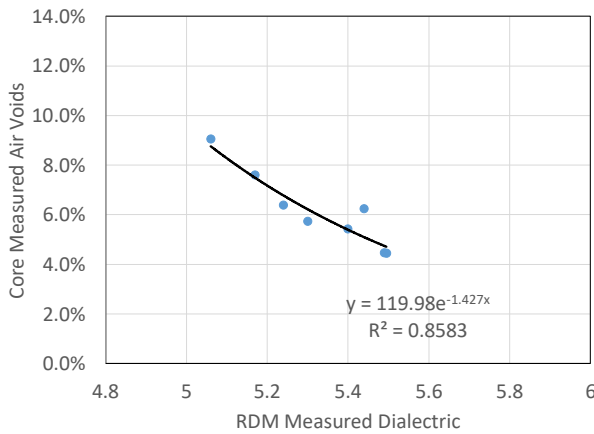
**Figure 34. Eyota, Minnesota Calibration Model for All Cores**



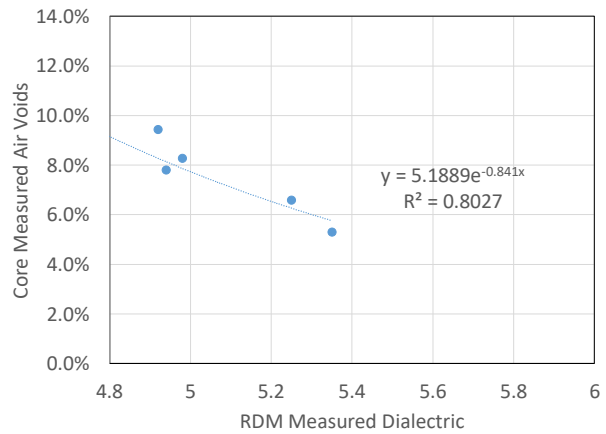
a. Section 1



b. Section 2



c. Sections 3 and 4



d. Sections 5 and 6

**Figure 35. Core Measured Air Voids vs. Ground Penetrating Radar Dielectrics for Individual Sections of HW14**

The results of this survey were used for both real time and post-construction investigations of HMA compaction levels. During the survey, the dielectric data collected were used to make general estimations of the relative achieved compactions. Real-time results were communicated to the contractor to provide information on how roller patterns and mix changes were affecting compaction levels. No action was taken based on the field interpretations communicated to the contractor, but the information was received positively and there is a possibility it could be used to greater effect during future RDM surveys.

A post-construction evaluation involved comparison of the dielectric data collected from different sections and locations. Two groups of data were extracted for each section:

- “Mainline” data collected from 4 to 8 ft away from the longitudinal joint.
- “Joint” data collected on the confined side of a joint from 0 to 3 inches away from the joint. These data are available only for Sections 1, 2, 4, and 6.

These data, as well as the corresponding air void contents calculated using the calibration model shown on Figure 29, were used to evaluate the effect of design mix and construction practices on the achieved level of compaction. Table 15 and Table 16 present mean and median values of dielectric constants and air void contents, respectively, for each section joint and lane.

**Table 15. Mean and Median Dielectrics for Mid-lanes and Joints**

Section	Dielectric			
	Lane		Joint	
	Median	Mean	Median	Mean
1	5.23	5.23	5.06	5.07
2	5.39	5.4	5.28	5.29
3	5.29	5.29	N/A	N/A
4	5.38	5.38	5.35	5.35
5	5.28	5.28	N/A	N/A
6	5.22	5.22	5.2	5.2

Note:

N/A = not applicable

**Table 16. Mean and Median Air Void Contents for Mid-lanes and Joints**

Section	Air Voids, Percent			
	Lane		Joint	
	Median	Mean	Median	Mean
1	6.61	6.66	7.73	7.7
2	5.70	5.69	6.31	6.3
3	6.25	6.25	N/A	N/A
4	5.75	5.77	5.91	5.95
5	6.31	6.34	N/A	N/A
6	6.67	6.68	6.79	6.79

Analysis of Table 15 and Table 16 shows that the control section (3 rollers, 3/4-inch maximum aggregate size) resulted in the lowest mean dielectric constants and the highest air void contents for both mid-lane and joint. Sections 2, 3, and 6 differ from Section 1 by only one factor (number of roller passes, maximum aggregate size, or presence of Evotherm). It was observed that an addition of Evotherm for the same mix design (Section 6) improved compaction of the joint, but did not improve compaction in the mainline. The addition of a fourth roller (Section 2) greatly improved the mean air void content in the mainline, but an improvement in the mean air void content for the joint was not as significant. The reduction in the maximum aggregate size (Section 3) resulted in a moderate reduction in the mean air void contents for the mainline.

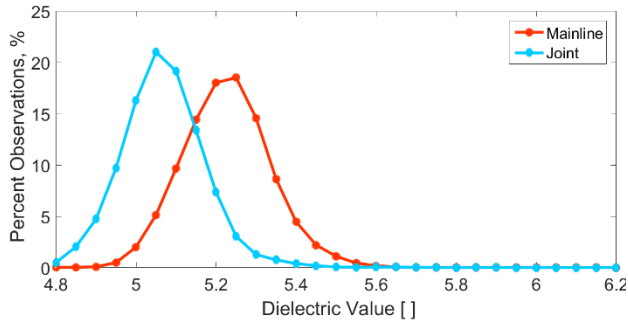
Sections 3 and 5 had the same HMA mix with a smaller (1/2 inch) maximum aggregate size, but Section 5 also had Evotherm in the HMA mix. Tables 15 and 16 show that Evotherm did not

improve compaction in the mid-lane for this mix design, as was observed for the HMA mix with a larger maximum aggregate size. Since no RDM data was available for Section 5 joint, an effect of Evotherm additive on compaction at the joint could not be evaluated.

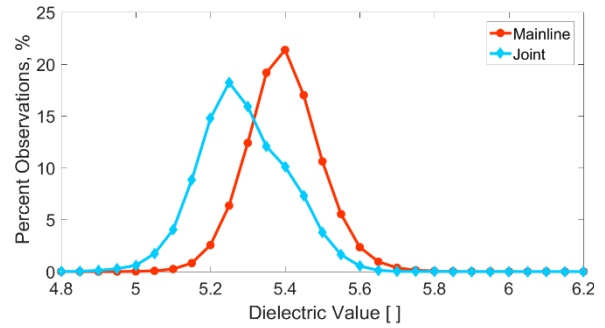
Finally, the use of a mix with a smaller maximum aggregate size and four-roller passes for Section 4 resulted in the same HMA compaction in the mid-lane as for Section 2, but a much better compaction level at the joint. Based on this conclusion, it was determined that this combination of mix design and construction practice resulted in the best overall compaction among all the sections in this demonstration project.

Figure 36 and Figure 37 show frequency distributions of the RDM-measured dielectric constants and corresponding air void contents, respectively. The analysis of these figures confirms the conclusions made from the analysis of Table 15 and Table 16. Also noted was that the compaction near joint is worse than in the middle of the lane for Sections 1 and 2, where the HMA mix with the maximum aggregate size of 3/4 inch was used. However, the use of a smaller maximum aggregate size or Evotherm additive significantly reduced the difference in compaction levels between the mid-lane and joint.

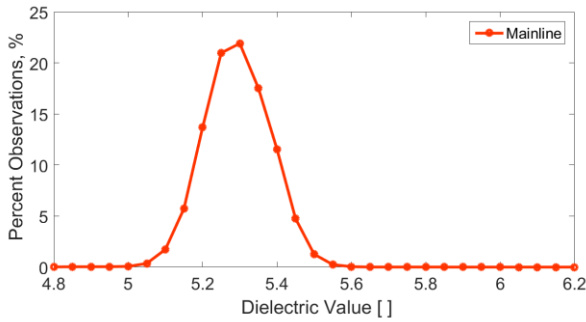
Finally, Figure 37f suggests that almost the entire Section 4 exhibited the air void levels lower than 8 percent, which indicates a very good compaction. All six cores extracted from Section 4 resulted in the laboratory-determined air void contents lower than 8 percent, including the core taken near the joint. Therefore, the core measured air void data confirms the RDM assessment results.



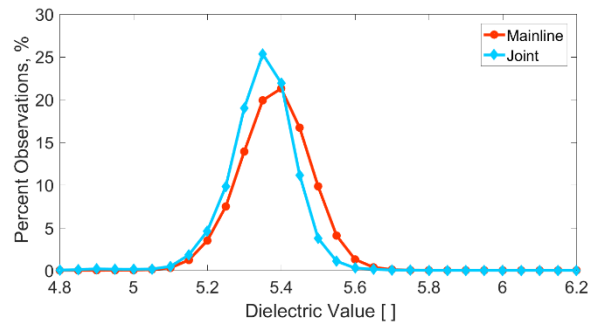
A. Section 1



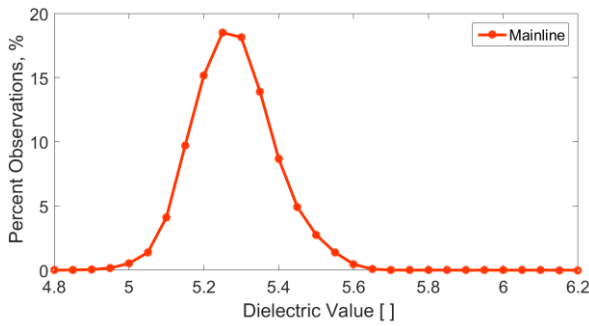
B. Section 2



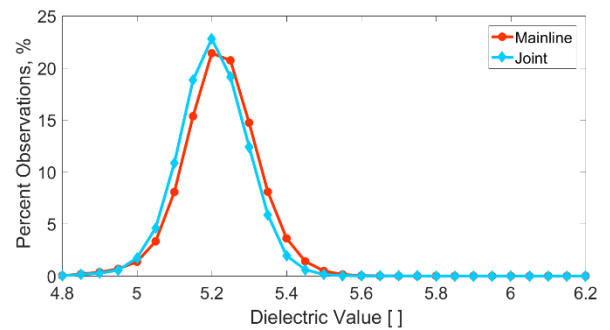
C. Section 3



D. Section 4

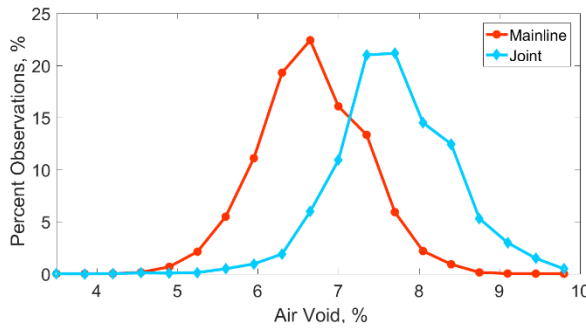


E. Section 5

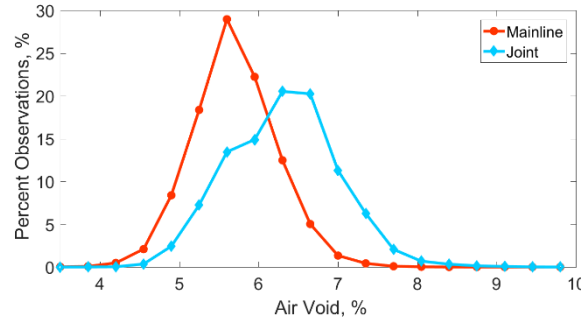


F. Section 6

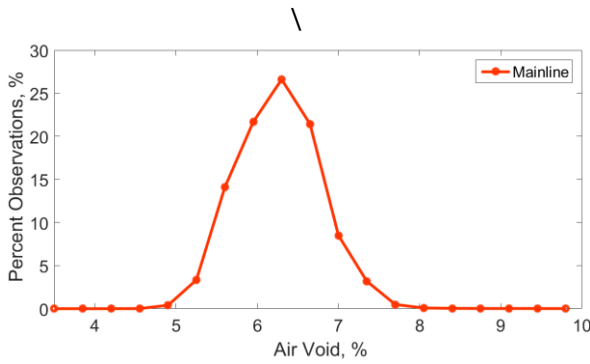
**Figure 36. Frequency Distributions of the Rolling Density Meter-measured Dielectric Constants for HWY 14 Sections near Eyota, Minnesota**



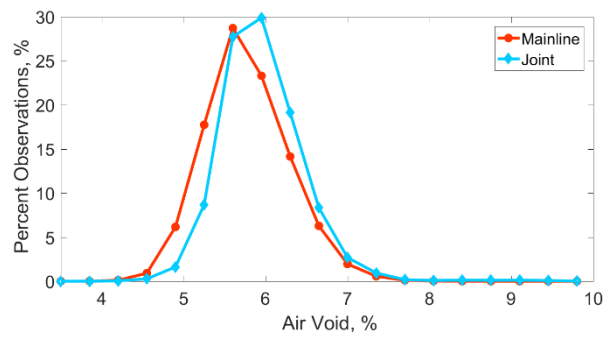
A. Section 1



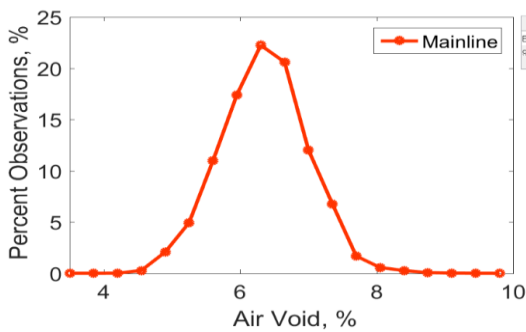
B. Section 2



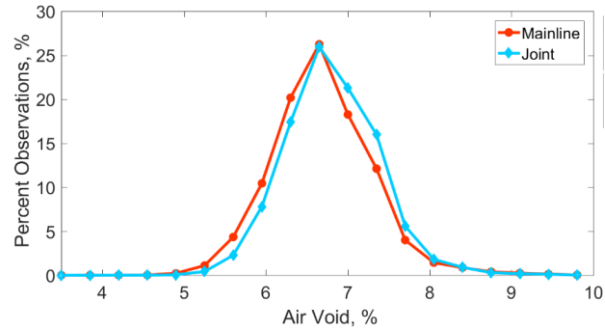
C. Section 3



D. Section 4



E. Section 5



F. Section 6

**Figure 37. Frequency Distributions of the Rolling Density Meter -measured Air Void Contents for HWY 14 Sections near Eyota, Minnesota**

## 5.0 Conclusions and Recommendations

Early deterioration and long-term performance of HMA pavements are highly affected by the quality of compaction. To minimize potential delay in traffic closure on rehabilitation of heavily-trafficked areas where quality of compaction is especially important, it is desirable that

the measurements be taken immediately after final roller compaction, while providing high pavement coverage. Traditional compaction determination methods, such as coring or nuclear density gauge testing, do not provide fast and continuous data collection. Fast, non-destructive and continuous technology is required to meet these demands. A rolling density meter, the GPR-based device that addresses the recommendations of SHRP2, has proved to be a promising tool for real-time assessment of relative compaction and post-survey analysis of the achieved air void content.

A series of demonstration projects with the RDM equipment was conducted in Minnesota, Maine, and Nebraska. These field trials were used to independently evaluate the RDM technology and to develop a recommended methodology for data collection. The surveys were conducted over hundreds of miles of pavement constructed with various mix designs and construction practices. The experiences of these surveys were used to develop a recommended protocol for the collection of RDM data and cores. The protocol included recommendations related to the following:

- Standardization of the survey file parameters to allow continuity between projects and agencies as well as convention for data organization.
- Survey wheel calibrations to ensure agreement between RDM data and construction data.
- Survey segment length selection to avoid interfering with paving operation while maintaining the pace of the paving operation.
- Evaluation of the GPR sensors precision and bias through the collection of randomized datasets.
- Survey patterns that provide the data most critical to determining compaction while minimizing the number of passes.
- A core collection protocol to ensure that cores are spatially distributed through the survey area and represent the full range of dielectric values.

This protocol helped the RDM survey team to collect real-time relative compaction data in critical locations without interfering with paving operations. These real-time data were used during the case studies to inform the paving crew of relative compaction trends and thus to influence the paving operation. In one of the demonstration projects, consistent compaction deficiencies near roller pattern changes were identified. This information was shared with the paving crew and the issue was addressed.

While the RDM surveying can be used without core collection to provide relative compaction assessment, calibration cores are required to convert the dielectric values into air void estimates. The quality of the calibration model is highly influenced by the uncertainty associated with air void estimates. The proposed core data collection protocol involves taking hundreds of measurements directly over the core and the immediate location of the core. It has been shown

to produce accurate measurements of the dielectric at the core location and has resulted in good calibration models capable of making air void estimates with low uncertainty. Calibration models produced using this method typically have  $R^2$  values ranging from 0.80 to 0.95.

The results of the trial implementation show the ability of the method to assess relative compaction levels non-destructively, and at a greater coverage and speed than traditional methods allow. By collecting data along the entire paved area, the conclusions can potentially be used as QC of compaction efforts and to determine the most critical aspects of achieving improved as-built density in HMA pavement construction through comparison with other performance measures and construction practice measurements.

The demonstration projects and analyses performed during this study showed the potential of RDM surveying to provide continuous non-destructive data on compaction. Although the results were promising, further improvements in several areas may benefit the implementation of this technology.

First, the protocol developed in this project was primarily designed to address the needs of MnDOT, with additional input from Maine and Nebraska DOTs. The protocol was intended to provide information considered most critical by these participating DOTs. Other agencies may have other needs requiring modifications of the survey procedures.

RDM surveying still requires the collection of cores for calibration of the dielectric versus air voids model. Cores are expensive, time consuming and destructive, so eliminating coring would greatly benefit the RDM surveying. Also, coring is difficult on extremely thin lifts. While the RDM can be used on very thin lifts for relative compaction assessment, without core collection, the dielectric values cannot be converted into air voids. Further research into empirical models relating pavement mix volumetrics to dielectric response or the use of test calibration sections should be pursued.

This study concentrated on the evaluation of accuracy and productivity of the RDM device. Although the results of this study confirm a great potential of the RDM to provide nondestructive, accurate, and high coverage assessment of compaction uniformity, to facilitate the implementation of this technology, it is important to develop best practices for QA and QC applications.

## 6.0 References

Al-Qadi, I. L. and S. Lahouar. 2005. "Measuring layer thicknesses with GPR—Theory to practice." *Construction and Building Materials* 19.10: 763-772.

Al-Qadi, I.L., D.K. Ghodgaonkar, V.K. Varada, and V.V. Varadan. 1991. "Effect of moisture on asphaltic concrete at microwave frequencies." *IEEE Transactions on Geoscience and Remote Sensing* 29.5: 710-717.

- Al-Qadi, I. L., S. Lahouar, and A. Loulizi. 2001. "In situ measurements of hot-mix asphalt dielectric properties." *NDT & e International* 34.6: 427-434.
- Al-Qadi, I., Z. Leng, S. Lahouar, and J. Baek. 2010. "In-place hot-mix asphalt density estimation using ground-penetrating radar." *Transportation Research Record: Journal of the Transportation Research Board* 2152: 19-27.
- Bonnaure, F., G. Gest, A. Gravois, and P. Uge. 1977. "A New Method of Predicting the Stiffness of Asphalt Paving Mixtures." *Proceedings of the Association of Asphalt Paving Technologists*, Vol. 46, pp. 64–104.
- Evans, R., M. Frost, M. Stonecliffe-Jones, and N. Dixon. 2008. "A review of pavement assessment using Ground Penetrating Radar (GPR)," *Proceedings of the 12th international conference on Ground Penetrating Radar, Birmingham, UK*.
- Hoegh, K., Khazanovich, L., Dai, S., and H.T. Yu. 2015. "Evaluating asphalt concrete air void variation via GPR antenna array data." *Case Studies in Non-destructive Testing and Evaluation*: 27-33.
- Kassem, E., A. Chowdhury, T. Scullion, and E. Masad. 2012. "Measurements of asphalt pavement density using ground penetrating radar and its relationship to performance." *Transportation Research Board 91st Annual Meeting*. No. 12-4051.
- Lai, W., T. Kind, S. Kruschwitz, J. Wöstmann, and H. Wiggenhauser. 2014. "Spectral absorption of spatial and temporal ground penetrating radar signals by water in construction materials," *Non-destructive Testing Evaluation International*, Vol. 67, pp. 55-63.
- Leng, Z. 2011. "Prediction of In-Situ Asphalt Mixture Density Using Ground Penetrating Radar: The Theoretical Development and Field Verification," Ph.D. Thesis, University of Illinois at Urbana-Champaign, USA.
- Leng, Z. and I.L. Al-Qadi. 2014. "An innovative method for measuring pavement dielectric constant using the extended CMP method with two air-coupled GPR systems." *NDT & e International* 66: 90-98.
- Leng, Z., I. L. Al-Qadi, and S. Lahouar. 2011. "Development and validation for in situ asphalt mixture density prediction models." *NDT & e International* 44.4: 369-375.
- Linden, R. N., Joe P. Mahoney, and Newton C. Jackson. 1989. "Effect of compaction on asphalt concrete performance." *Transportation Research Record* 1217.
- Maser, K. and A. Carmichael. 2015. *Ground Penetrating Radar Evaluation of New Pavement Density*. No. WA-RD 839.1.
- Pellinen, T. K., Jiansheng Song, and Shangzhi Xiao. 2004. "Characterization of hot mix asphalt with varying air voids content using triaxial shear strength test." *Proceedings of the 8th Conference on Asphalt Pavements for Southern Africa (CAPSA'04)*. Vol. 12.

Popik, M., K. Maser, and C. Holzschuher. 2010. "Using high-speed ground penetrating radar for evaluation of asphalt density measurements." *Annual conference & exhibition of the transportation association of Canada*, Canada.

Saarenketo, T. and T. Scullion. 2000. "Road evaluation with ground penetrating radar." *Journal of Applied Geophysics* 43.2: 119-138.

Saarenketo, T. and P. Roimela. 1998. "Ground penetrating radar technique in asphalt pavement density quality control." *Proceedings of the seventh international conference on ground penetrating radar*. Vol. 2.

Scott, M. L., N. Gagarin, M.K. Mills, and M. Oskard. 2006. "Step Frequency Ground Penetrating Radar Applications to Highway Infrastructure Measurement and System Integration Feasibility with Complementary Sensors." *AIP Conference Proceedings*.: 1, 1624-1631.

Scullion, T. and Y. Chen. 1999. Using Ground-Penetrating Radar for Real-Time Quality Control Measurements on New HMA Surfaces, Report 1702-5, Texas Transportation Institute.

Sebesta, S., T. Scullion, and T. Saarenketo. 2013. *Using infrared and high-speed ground-penetrating radar for uniformity measurements on new HMA layers*. Transportation Research Board.

Shang, J. Q., J. A. Umana, F. M. Bartlett, and J. R. Rossiter. 1999. "Measurement of Complex Permittivity of Asphalt Pavement Materials." *Journal of Transportation Engineering* 125.4:347-56.

Shangguan, P. and I. L. Al-Qadi. 2014. "Content-based image retrieval approaches to interpret ground penetrating radar data." *Construction and Building Materials* 69: 10-17.

Shangguan, P. and I. L. Al-Qadi. 2015. "Calibration of fdtd simulation of gpr signal for asphalt pavement compaction monitoring." *IEEE Transactions on Geoscience and Remote Sensing* 53.3: 1538-1548.

Wilson, B. T. and S. Sebesta. 2015. "Comparison of Density Tests for Thin Hot-Mix Asphalt Overlays." *Transportation Research Record: Journal of the Transportation Research Board* 2504: 148-156.

Witczak, M. and O. Fonseca. 1996. "Revised predictive model for dynamic (complex) modulus of asphalt mixtures." *Transportation Research Record: Journal of the Transportation Research Board* 1540: 15-23.